The Role of PJA2-CDK5R1 in β-cell Function

Yasir Mohamud

A thesis submitted to the Faculty of Graduate and Postdoctoral Studies in partial fulfillment of the requirements for the M.Sc. degree in Biochemistry

Department of Biochemistry Microbiology and Immunology
Faculty of Medicine
University of Ottawa

Abstract

Diabetes is a global epidemic characterized by an inability to control blood glucose due to lack of insulin secretion and/or regulation. The International Diabetes Federation (IDF) estimates approximately 382 million people worldwide to be affected by diabetes and domestically, the Canadian Diabetes Association estimates approximately 9 million diabetic/pre-diabetics. The protein Cdk5r1/p35 negatively regulates insulin secretion and thus can be targeted as a novel therapy for diabetes. Immunoprecipitation coupled with mass spectrometry has identified candidate interactors of p35. Using high throughput RNAi screening, candidate genes were knocked down with target shRNA and p35 protein levels were monitored. The screen identified RPAP3 as a potential regulator of p35 levels. Knockdown of RPAP3 increased p35 protein levels however insulin secretion was unaffected suggesting a more complex model. In the same manner, PJA2 was identified as the E3 ligase responsible for p35 ubiquitination and subsequent degradation. With the preface that PJA2 undergoes auto-ubiquitination, site-directed mutagenesis was employed to generate lysine to arginine mutants in an effort to identify auto-ubiquitination sites. Mutating lysines K642, K657, and K666 (K3R) causes PJA2 stabilization and reduced auto-ubiquitination compared to wild-type. In vitro ubiquitination assays demonstrate that K3R is functional and can ubiquitinate GST-p35. However, overexpression of PJA2 in Min6 cells is associated with poor regulation of insulin secretion. Co-immunoprecipitation experiments reveal that PJA2 undergoes self-interaction. PJA2-p35 interaction is further characterized by demonstrating that p25 is sufficient to interact with PJA2. Furthermore, PJA2-p35 dynamics may affect PJA2 auto-ubiquitination capacity.

Acknowledgment

First and foremost, I would like to thank my thesis supervisor Dr. Robert Screaton for giving me the opportunity to study in his lab, the guidance he has provided, as well as the freedom to pursue my scientific curiosities. I would like to give special thanks to members of the Screaton lab past and present for being brilliant colleagues and inspiring people. I would also like to thank the people of CHEO RI for providing the best environment for learning, research, and above all a sense of community. Finally, I would like to thank my family and wonderful parents for all their support.

Table of Contents

Chapter 2: Methods

Chapter 3: Results

List of Abbreviations

3’ UTR	3 prime untranslated region
ADP	Adenosine diphosphate
AKAP	A-Kinase Anchor Protein
AKT	Protein Kinase B
AMP	Adenosine monophosphate
AMPK	Adenosine monophosphate kinase
β -cell	Beta cell
ATP	Adenosine triphosphate
CAMKK2	Calcium/calmodulin-dependent protein kinase kinase 2
CD4+	Cluster of differentiation 4 positive
CD8+	Cluster of differentiation 8 positive
CDK5	Cyclin-dependent kinase 5
CDK5R1/p35	Cyclin-dependent kinase 5 regulatory subunit 1
CDK5R1AP3	Cyclin-dependent kinase 5 regulatory subunit 1 associated protein 3
Clec16a	C-type lectin domain family 16
E1	Ubiquitin-activating enzyme
E2	Ubiquitin-conjugating enzyme
E3	Ubiquitin protein ligase
ER	Endoplasmic Reticulum
G6P	Glucose-6-phosphate
GLUT2	Glucose transporter 2
GST	Glutathione-S-Transferase

HECT	Homologous to the E6-associated protein carboxyl terminus
HEK293T	Human embryonic kidney 293 T-antigen
HFD	High-fat diet
Hrd1	ERAD-associated E3-ubiquitin protein ligase
IL-1β	Interleukin- 1β
IRS-1	Insulin receptor substrate 1
LKB1	Liver kinase B1
Mdm2	Mouse double minute 2 homolog
MdmX	Mouse double minute 4 homolog
MHC	Major histocompatibility complex
Min6	Mouse insulinoma 6 (mouse pancreatic beta cell line)
Mob1	Mps one binder 1
Munc18-1	Mammalian uncoordinated 18-1
NADH	Nicotinamide Adenine Dinucleotide
NOGO	Neurite outgrowth inhibitor
Nrdp1	Neuregulin receptor degradation protein 1
p53	tumor protein 53
PJA2	Praja2, also known as Neurodap1
PKA	Protein Kinase A
PMP	Pancreatic multipotent precursors
POMC	Pro-opiomelanocortin
RING	Really Interesting New Gene
RNA	Ribonucleic acid
RNAi	RNA interference

SDS-PAGE	Sodium Dodecyl Sulfate Polyacrylamide Gel Electrophoresis
shRNA	short-hairpin RNA
SIK2	Salt-inducible kinase 2
TAK1	Transforming growth factor β activated kinase 1
TCA	Tricarboxylic acid cycle
TNFα	Tumor necrosis factor alpha
TORC2	Transducer of regulated CREB protein 2
UBD	Ubiquitin binding domain
UFBP1	UFM1-binding protein 1 containing a PCI domain
UFL1	UFM1-specific ligase 1
UFM1	Ubiquitin fold modifier 1
UPS	Ubiquitin Proteasome System
VDCC	Voltage-dependent calcium channel

List of Figures and Illustrations

List of Appendices

Chapter 1: Introduction

Diabetes

The word diabetes stems from Greek origin translating to 'pass through' or 'siphon' referencing the nature of the disease to generate excessive discharge of urine. Relatedly, the word mellitus can be translated as "sweet honey" in reference to the increased presence of glucose in the urine and blood of diabetics. In fact, diabetes was among the first diseases to be characterized dating as far back as 1552 BCE and for 3 millennia the prognosis of the disease has been bleak. It was not until 1921 when Frederick Banting and Charles Best used the first insulin extracts to treat diabetic canines that an underlying understanding of the disease emerged (1). It ultimately came to light that insulin, a hormone produced in pancreatic β-cells, plays a key role in mediating glucose uptake in skeletal muscle, hepatic and adipose tissue and consequently regulating blood glucose [reviewed in (2)]. β-cells situated in the islets of Langerhans can be subjected to autoimmune assaults or undergo insulin-resistance mediated exacerbation leading to Type I or II diabetes respectively. The current treatments for diabetes attempt to re-introduce external insulin through multiple daily injections or alleviate insulin resistance through oral medication. Islet transplantations have shown promising results however due to islet graft death or loss of function this treatment approach is not permanent and requires a lifetime dependence on immunosuppressant to prevent graft rejection (3-5). Understanding the mechanisms behind β-cell dysfunction will be crucial for developing novel therapeutic approaches for treating diabetes.

Type I Diabetes

Diabetes has classically been subcategorized into Types I or II due in part to the fundamental differences in the etiology of the disease. Type I, also called insulin-dependent or juvenile diabetes, was linked to abnormalities in β-cells as early as 1965 through morphological analysis of the islets of Langerhans (6). This form of diabetes accounts for approximately 10% of all cases and is predominantly diagnosed during childhood or adolescence. Type I diabetes can be separated into two distinct phases wherein the first phase, termed insulitis, is characterized by leukocytic invasion of islets. This auto-immune assault results in β-cell loss which ultimately leads to the second phase characterized by an inability to produce insulin and regulate glucose (7). The β-cell assault itself is mediated by T lymphocytes (T-cells; reviewed in (7-12)). In brief, β-cell destruction occurs when CD4+ and CD8+ T-cells infiltrate islets in response to β-cell upregulation of interferon alpha and subsequently MHC class I (8). The etiology of the disease is not entirely clear but it's evident that there is interplay between genetic and environmental factors.

Interestingly, Type I diabetes has been subcategorized into 3 distinct forms termed autoimmune, non-autoimmune fulminant (severe and sudden in onset) and non-autoimmune nonfulminant (chronic) (13). Autoimmune Type I diabetes demonstrated lymphocytic infiltration of pancreas, elevated class I MHC, and increased levels of autoantibodies. The non-autoimmune nonfulminant category does not demonstrate the above mentioned characteristics and is characterized by a slow progression of beta cell loss. Non-autoimmune fulminant is the most aggressive form of the disease whereby lymphocytic infiltration takes place in the exocrine pancreatic tissue. It is important to differentiate between the different

forms of Type I diabetes because it can ultimately guide our understanding of the disease and promote the development of better therapeutics.

Type II Diabetes

The Canadian diabetes Association (CDA) estimates there are 285 million diabetics worldwide and this number continues to increase. A recent study found a similar estimate for the global prevalence of diabetes and predicted this estimate to rise to 439 million by 2030 (14). Domestically, the CDA estimates approximately 9 million Canadians are diabetic or pre-diabetic. Type II diabetes is by far the most common form of the disease affecting more than 90% of all diabetics. Obesity and sedentary lifestyle have been linked to Type II diabetes and insulin resistance (15-23).

Obesity and Insulin Resistance

Obesity is a major factor implicated in the rising diabetes epidemic. Indeed many studies have demonstrated that obesity rates have increased in recent years (24-31). Interestingly, a study looking at adiposity gains across a 10-year period concluded that lean groups were able to maintain their weight whereas obese individuals gained significantly more weight (31). This increased propensity to accumulate fat could implicate a genetic component that promotes a cycle of weight gain. For instance, adipose tissues have been shown to secrete hormones such as resistin which can exacerbate the insulin resistance phenotype (32). Furthermore, obesity has been linked to a chronic state of inflammation whereby elevated levels of TNF-α can be observed in the adipose tissue of obese models (reviewed in (33)). The hormone insulin functions by binding to its designated receptor on insulin-responsive cells and triggers a signaling cascade whereby the insulin receptor phosphorylates itself and its substrates. Insulin resistance is a phenomenon characterized by

an inability of peripheral tissue to properly respond to insulin stimulation which results in elevated circulating insulin (34). Presence of TNF- α appears to hinder the insulin signaling pathway thus contributing to insulin resistance. Indeed it has been shown that high fat diet (HFD) and particularly saturated fatty acids such as palmitate promote inflammasome activation and subsequent production and secretion of caspase 1 and interleukin-1β (IL-1β) (35). The resulting inflammation caused impaired insulin signaling. Obesity has also been shown to cause endoplasmic reticulum (ER) stress and subsequent activation of inflammatory signaling pathways, further contributing to the insulin resistance phenotype (36, 37).

Interestingly, insulin resistance is increased during puberty and returns to normal afterwards (38). Similar effects were observed in the pregnant and elderly (reviewed in (19)) suggesting that insulin resistance may play a role in normal physiology. Nevertheless, the association of cardiovascular disease, hypertension, Type II diabetes and other elements of the metabolic syndrome point to a convincing pathological role for insulin resistance (39). Whether the pathology of insulin resistance is a global reduction in glucose uptake or tissue specific loss of insulin sensitivity remains to be fully understood. It is possible that the insulin resistance associated with metabolic syndrome may affect hepatic, muscle, and adipose tissues to varying degrees. Furthermore, prolonged insulin resistance and the concomitant appearance of hyperglycemia can have detrimental effects on β-cell health. In particular, poor insulin sensitivity can trigger a vicious cycle whereby β-cells hyper secrete insulin eventually succumbing to the increased demands.

Pancreatic β-cells

Parallels between β-cells and Neurons

Interestingly, there are striking similarities between β-cells and neurons. For example, both cell types can be classified as excitatory cells that use membrane depolarization to secrete either insulin in the case of pancreatic β-cells or neurotransmitters in neurons. In addition, researchers were able to demonstrate that approximately 15% of β-cell specific genes were also expressed in neurons (40-42). Furthermore, these genes corresponded to proteins important for synaptic vesicle formation and neurotransmitter transport. It is important to explore the parallels between neurobiology and β-cell biology because knowledge gained from either field can help to advance the other. Such was the case when researchers screened a library of neurogenic activators to identify a chemical that promotes pancreatic β-cell differentiation (43). In addition to the above-mentioned similarities, both β-cells and neurons are able to respond to changes in glucose concentrations demonstrating an underlying mechanism of glucose sensing.

Glucose Sensing

The basic function of pancreatic β-cells is to secrete insulin in response to glucose in order to maintain euglycemia. Consequently, β-cells have developed a precise mechanism, which allows them to sense glucose in their environment and respond by secreting the appropriate amount of insulin to facilitate glucose uptake in peripheral tissues. Similarly, it has been shown that certain neurons in the brain can act as glucose sensors. In particular, researchers identified two types of neurons that respond to changes in glucose levels by either increasing or decreasing their activity and they appropriately termed these neurons as glucose-excited or glucose-inhibited neurons respectively ((44, 45) reviewed in (46)). For

example, compromising the glucose-sensing ability of glucose-excited pro-opiomelanocortin neurons (POMC) by disrupting membrane depolarization leads to an impaired whole-body response to glucose (47). Furthermore, the researchers demonstrated the glucose-sensing POMC neurons became defective in an obese diabetic mouse model supporting the notion that POMC neurons could be playing an important role in regulating glucose levels.

Indeed, the mechanism by which pancreatic β-cells sense glucose is better characterized than neuronal glucose sensing. Briefly, glucose is transported into the β-cell through transmembrane glucose transporter 2 (GLUT2) followed by glucokinase –mediated phosphorylation. GLUT2 is specific to pancreatic β-cells, hepatocytes, and epithelial cells of the kidney and intestines (48-51). In addition, it demonstrates the highest capacity for glucose but the lowest affinity allowing it to uptake glucose only during times of abundance. However, the more important component of the glucose-sensing machinery is the rate-limiting step whereby glucose is phosphorylated by the glycolytic enzyme glucokinase (reviewed in (52)). For example, replacing GLUT2 with GLUT1 in pancreatic β-cells does not significantly affect the ability of the β-cell to respond to changes in extracellular glucose concentration. In contrast, changing glucokinase via gene transfer experiments to hexokinase 1 leads to loss of insulin promoter activity and responsiveness to changes in glucose concentrations (53).

Classical Model of Insulin Secretion

Following GLUT-2 mediated glucose transport and subsequent phosphorylation by glucokinase, the generated glucose-6-phosphate (G6P) becomes trapped in the β-cell where it enters the glycolytic pathway to be metabolized into pyruvate (reviewed in (52)). Both

glycolytic products pyruvate and NADH enter mitochondria as substrates of the tricarboxylic acid cycle (TCA) also known as the citric acid/ Krebs cycle to generate ATP. The resulting increase in ATP/ADP ratio leads to closure of ATP-sensitive K_{ATP} channels, membrane depolarization, voltage-dependent calcium channel (VDCC) activation resulting in Ca^{2+} influx and finally insulin secretion (reviewed in (35, 54, 55)).

Therapeutics of Diabetes

As mentioned previously, diabetes has classically been categorized into insulin-dependent Type I diabetes and insulin-independent Type II diabetes. The former characterized by β-cell destruction and the latter characterized by β-cell dysfunction both share the hallmark diabetes trait of hyperglycemia and its associated risk factors. Research for novel diabetes therapies is focused on two main approaches, namely generating an unlimited supply of functional β-cells for the purpose of transplantation or improving β-cell health and function.

Promoting β-cell Regeneration

A popular approach has been the use of stem cells to generate human pancreatic β-cells (56-60). Although promising, the main drawback to this strategy has been the lack of functional β-cells that are able to respond to glucose fluctuations with appropriate insulin secretion. Recently, Melton and associates successfully generated functional β-cells from human pluripotent stem cells (56). They further demonstrated that these stem cell derived β-cells are able to respond to multiple challenges of glucose stimulation by secreting insulin levels comparable to adult primary β-cells. Most promising, transplantation of these stem

cell derived β-cells into mice rapidly improved glucose control. The next steps would require developing an appropriate encapsulation platform to protect the β-cells from immune-mediated destruction. Of course, researchers have explored other avenues of β-cell regeneration such as promoting pancreatic multipotent precursors into β-cell lineage (61), but for the sake of brevity, these will not be discussed here.

β -cell Functional Compensation

The alternative therapeutic approach has been to improve the function of remaining β-cells. Fortunately, β-cells are able to compensate for the increased insulin demand and can hyper-secrete insulin to maintain glucose homeostasis and subsequently prevent or delay the onset of Type II diabetes. Compensation occurs when β-cells functionally increase insulin output or increase β-cells mass (62). Insulin resistance mediated compensatory increase in β-cell mass can be insufficient to ward off hyperglycemia (63). It is possible that β-cell proliferation may actually contribute to β-cell dysfunction as division may require suppressing function. In addition to increased mass and hypertrophy, β-cells are indeed capable of functional adaptation in response to obesity (64, 65). Consequently, focus on increasing functional output per β-cell rather than increasing the number of β-cells in order to maintain euglycemia becomes a worthwhile approach.

It is possible that insulin resistance emerges with age and the inability of the β-cell to compensate by secreting more insulin could initiate Type II diabetes (66). Examining the adaptive capability of β-cells could help to identify dysfunctional β-cells that predispose people to diabetes and generate novel treatment opportunities. Genetic variations predispose a subset of the population to be at greater risk for developing diabetes and this variation can help to identify genes with protective or detrimental roles. Recently, SIK2, a serine/threonine

kinase in the AMPK family, has been implicated in playing a protective role in β-cell function (65, 67). Interestingly, SIK2 levels are increased under high glucose conditions as well as models of metabolic syndrome and high-fat diet. Elevated SIK2 levels in β-cells lead to enhancement in insulin secretion thus compensating for dysfunctional glucose homeostasis. The recently elucidated mechanism involves SIK2 phosphorylation of the CDK5-activating protein p35 (CDK5R1) at Ser91. The CDK5-p35 complex has been shown to phosphorylate and consequently inhibit the VDCC leading to reduced calcium influx and insulin secretion (65, 68-70). SIK2 phosphorylation of p35 most likely enhances its ubiquitination and subsequent degradation by the ubiquitin/proteasome system however this has not yet been formally demonstrated. Furthermore, PJA2 has been implicated as the E3-ligase that directly ubiquitinates p35. Knockdown of PJA2 results in p35 elevation and reduction in insulin secretion whereas overexpression of wild-type PJA2 but not an E3-ligase mutant leads to decreased p35. Taken together, the novel signaling pathway of SIK2-p35-PJA2 increases pancreatic β-cell functional compensation.

AMPK Family in Pancreatic β-cells

Metformin is the number one prescribed oral anti-diabetic drug in the world. It functions in part by reducing hepatic glucose output while also enhancing glucose utilization. Metformin is able to activate the enzyme AMPK (AMP-activated protein kinase); a heterotrimer composed of an α, β, and γ subunit (71). The catalytic α-subunit along with the β/γ regulatory subunits of this enzyme work in unison to generate a cellular energy sensing complex capable of regulating several key metabolic pathways (72). More specifically, AMPK is able to detect fluctuations in the AMP: ATP ratio. Briefly, AMP and ADP

allosterically bind key sites on γ regulatory subunit to induce conformational changes, thus exposing an active site (Thr-172) on the α subunit. Phosphorylation of Thr-172 by upstream kinases such as LKB1, CAMKK2, and TAK1 leads to activation of AMPK (73-75). Furthermore, conformational changes prevent dephosphorylation to favor prolonged AMPK activity (76, 77). Following an increase in AMP and ADP levels and subsequent activation of AMPK, several key substrates are phosphorylated to conserve cellular energy and dictate metabolic flux. AMPK ultimately regulates the metabolic switch from energy consuming pathways such as protein and fatty acid synthesis to energy producing pathways such as fatty acid oxidation. Interestingly, the exact role of AMPK activation in β-cells is unclear. Acute activation of AMPK with the AMP analog AICAR showed contradictory results with regards to insulin secretion (reviewed in (55)). On the contrary, long-term AMPK activation either by pharmacological agents or overexpression of constitutively activate AMPK demonstrates insulin secretion impairment.

The Role of SIK2 in Pancreatic β-cells

SIK2 is a member of the AMPK family that plays a role in regulating TORC2 translocation by phosphorylating TORC2 at Ser171 and thus enhancing the interaction of TORC2 with 14-3-3 proteins (78). Furthermore, SIK2 mediated phosphorylation of TORC2 leads to its ubiquitination and degradation by the ubiquitin proteasome system (79). Interestingly, SIK2 mediated phosphorylation of p35 at Ser91 is also associated with its ubiquitination and degradation (65). SIK2 is also capable of phosphorylating Ser789 of IRS-1 (insulin receptor substrate 1); a substrate that is also regulated by the ubiquitin proteasome system (80). Considering that SIK2 is activated through the actions of insulin (via AKT2) (79) and insulin mediates IRS-1 degradation (81), one can hypothesize that SIK2

phosphorylation of IRS-1 could contribute to its UPS mediated degradation. It is clear that SIK2 plays an important role in bioenergetics. Indeed, SIK2 is stabilized by glucose and promotes insulin secretion in pancreatic β-cells. In fact, mice with β-cell specific ablation of SIK2 secrete less insulin and are glucose intolerant (65). Whether SIK2 overexpression can promote β-cell function remains to be tested.

Role of CDK5R1 (p35) in Neurons and β cells

CDK5R1, henceforth referred to by its more common name p35 (protein of 35 kDa mass), is an activator for the serine/threonine kinase CDK5. P35 is precisely regulated through several mechanisms that govern its expression level, translation, protein function, cellular localization, and ultimately its turnover. Indeed, it has been shown that microRNA, specifically miR103 and miR107, regulate p35 transcript levels by targeting the 3' UTR(82). Moreover, loss of miR107 shows the trend of increased p35 mRNA association with polysomal fractions suggesting increased translational efficiency. Interestingly, the 3' UTR of p35 mRNA is exceptionally large and bioinformatics analysis demonstrates the presence of AU-rich elements that play a role in destabilizing p35 transcript levels (83) .

The mechanism of p35 regulation in β-cells is not fully understood. For example, neuronal p35 can be cleaved by calpain to a truncated 25 kDa protein (p25), which demonstrates enhanced capacity to activate CDK5 (84). Furthermore, p25/CDK5 complex hyperactivity leads to increased phosphorylation of CDK5 substrates such as TAU, which play an important role in regulating cytoskeletal elements in neurons. Interestingly calcium influx in neurons induces calpain-mediated cleavage of p35 to p25. Moreover, it has been reported that p25 accumulates in the brains of Alzheimer patients (85). The p35/CDK5

complex in β-cells phosphorylates Ser783 of the VDCC channel and reduces calcium influx. However, it's unclear if intracellular calcium levels or calcium influx affects p35 in β-cells (65, 70). Furthermore, it's unknown whether p35 in β-cells can be cleaved or if the CDK5/p25 complex in β-cells would have increased activity and deregulation. Proteomic analysis has shown that p35 interacts with the E3 ligase PJA2 and shRNA mediated knockdown of PJA2 leads to p35 stabilization (65). Remarkably, p35 proteomics demonstrated an enrichment of E3 ligases identifying as many as 7 E3 ligases/components of E3 ligases. Furthermore, knockdown of multiple E3 ligases, namely PJA2 and HUWE1 resulted in significant elevation of p35 levels. These intriguing findings bring into question the specificity of E3 ligases. Indeed it is possible that p35 can undergo regulation by multiple E3 ligases in different contexts.

As previously mentioned, cleavage of p35 generates an N-terminal p10 fragment and a C-terminal p25 fragment. The p25 fragment is sufficient to bind CDK5 and also demonstrates enhanced capacity to activate the kinase. Furthermore, p25 cellular distribution is deregulated due in part to the loss of a myristoylation signal located on the N-terminal fragment of p35. It has been shown that both CDK5 activators p35 and p39 undergo myristoylation, which is dependent on the second glycine residue, and lysine clusters both of which are found on the N-terminal p10 fragments. Furthermore, this myristoylation event is important for p35/p39 membrane association because mutation of the myristoylated glycine residue to alanine promotes nuclear localization of p35/p39 (86). Interestingly, this membrane association has been shown to facilitate the calpain-mediated cleavage and proteasomal degradation of p35 and p39.

Role of CDK5 in β-cells

CDKs are cyclin-dependent serine/threonine kinases that are genuine regulators of cell cycle progression and require activator proteins called cyclins (reviewed in (87)). CDK5 has been called an atypical CDK in the sense that it does not affect the cell cycle. Contrary to this, the CDK5-p25 complex has been shown to phosphorylate retinoblastoma and consequently regulate cell cycle progression and apoptosis in neurons (88). Even so, CDK5 activity is widely regarded as being essential in post-mitotic neurons where it has been shown to regulate neuronal development, neurite outgrowth and migration, cytoskeletal dynamics, and secretion (56, 57). In fact, CDK5 plays such an important role so much so that genetic ablation results in perinatal lethality (39, 89). Within the past decade, it has come to light that CDK5 has extra-neuronal functions and in particular plays a critical role in pancreatic β-cells. Both CDK5 activators p35 and p39 are expressed in β-cells (68). Unlike the p35/CDK5 complex, which has been shown to play a negative role in insulin secretion, p39/CDK5 demonstrated the opposite phenotype. The proposed mechanism of p39/CDK5 involves phosphorylation of the synaptic protein MUNC18-1 that results in insulin vesicle fusion with the plasma membrane (68). Interestingly, CDK5 activity increases after glucose stimulation due to elevated p35 mRNA and protein levels (59). It is possible that following glucose-stimulated insulin secretion (GSIS), the cell requires a mechanism to attenuate calcium influx and reduce insulin secretion to basal levels. Indeed Wei et al. demonstrated that the p35-CDK5 complex attenuates Ca^{2+} influx and insulin secretion through inhibitory phosphorylation of L-type VDCC channel (70).

Ubiquitin Proteasome System

The ubiquitin proteasome pathway is a prevailing system built into the fabric of the cell and ultimately plays the role of dictating the ebb and flow of cellular function most notably through protein degradation. In 1975, Schlesinger and Goldstein reported on a 74 amino acid protein they appropriately termed ubiquitin due to its widespread presence in all animal cells (90). The importance of this protein was recognized in 2004 when Ciechanover, Hershko, and Irwin were awarded the Nobel Prize in Chemistry for their contributions to the study of ubiquitin-mediated protein degradation.

The underlying mechanism of ubiquitin-mediated degradation is an elegant two-part system whereby proteins are initially targeted through conjugation with multiple chains of an 8.5 kDa ubiquitin protein after which the protein is recognized and degraded into smaller peptides by the 26S proteasome (reviewed in (91)). Before protein degradation can take place, a series of 3 enzymes must initially activate, transport, and ultimately tag the ubiquitin moiety onto the substrate protein. The first enzyme, termed E1, is an ATP-dependent activating enzyme that functions in two steps. E1 binds ATP and ubiquitin and catalyzes the generation of ubiquitin-adenylate intermediate followed by the thioester-linkage of ubiquitin to an active cysteine on E1. The next enzyme in the chain termed E2 ubiquitin-conjugating enzyme is responsible for transferring the activated ubiquitin from the E1 to an active cysteine site on E2. Lastly, an E3 ubiquitin-ligase enzyme will bind both the E2 and its substrate and mediate the transfer of the ubiquitin moiety to a lysine residue on the substrate proteins [Reviewed in (92-96)].

The specificity of the ubiquitin proteasome system is dictated by the E3 ligase. E3-ligases are sub-categorized into three classes termed HECT, RING, or U-box. The first class,

termed HECT for homologous to the E6-associated protein carboxyl terminus, consists of approximately 30 proteins all of which possess an evolutionarily conserved cysteine residue. This residue generates a thiolester-intermediate with ubiquitin before it can be transferred to the substrate protein. The second class of E3 ligases and by far the most common among the three was termed RING for "Really Interesting New Gene" by Lovering et al. in 1992 (97). At the time, the zinc finger motif was merely thought to coordinate DNA binding. It quickly emerged that these RING domain proteins play an important role in the ubiquitin proteasome system. The RING domain itself is composed of eight cysteine and histidine amino acid ligands which coordinate interaction with two zinc atoms. The arrangement of the cysteine/histidine ligands can be either $C_3H_2C_3$ (termed RING-H2) or C_3HC_4 (termed RING-HC). A third class termed U-box E3 ligases can be considered a modified RING domain.

As previously mentioned, the ubiquitin proteasome system is engrained in the fabric of cell biology and the β-cell is no exception. For example, treatment of β-cells with the proteasome inhibitor MG132 resulted in reduced GSIS. This effect was due to aggregate formation of the glycolytic enzyme glucokinase (89). Another study looking at proteasome inhibition in MIN6 cells concluded that the UPS regulates insulin secretion by maintaining VDCC function and proper Ca^{2+} influx (98). In particular, the α-subunit of the VDCC channel can undergo ubiquitination. In addition, the UPS has also been shown to regulate the biogenesis of K_{ATP} channels and their surface expression in β cells (99, 100). Lastly, the UPS may be responsible for degrading misfolded aggregates which accumulate in β cells due to islet amyloid polypeptide depositions (100).

The Role of E3 Ligases in β-cell Function

The ubiquitin-proteasome system is all governing and demonstrates no tissue discrimination in its reign of protein degradation. Naturally, β-cells would be encompassed and β-cell function subject to UPS regulation. It has been established that E3 ligases confer specificity to the UPS and may play important roles in β-cell function, namely insulin secretion. For example, insulin secretion occurs when insulin-containing granules from a readily releasable pool fuse to the plasma membrane in SNARE-dependent manner. Therefore, exocytosis of insulin from β-cells requires proper formation of the SNARE complex. Tomosyn is a protein that negatively affects exocytosis by reducing SNARE complex formation. In fact, overexpression of tomosyn-1 or 2 reduces insulin secretion from pancreatic β-cells (99, 101-103). Furthermore, tomosyn-2 is glucose-responsive such that elevated glucose levels promotes tomosyn-2 phosphorylation, ubiquitination and subsequent degradation (61). The authors demonstrate that the E3 ligase Hrd1 is responsible for ubiquitination of tomosyn-2. In another study, pancreas-specific deletion of the E3 ligase HUWE1 led to p53-mediated β-cell apoptosis, decreased β-cell mass and reduced insulin secretion (104). Interestingly, the Type I diabetes susceptibility gene Clec16a is required for glucose-stimulated insulin secretion. In addition, pancreas specific ablation of Clec16a results in reduced ATP levels and oxygen consumption. Not surprisingly, these defects are associated with abnormal mitochondria in β-cells (102). The function of Clec16a is unclear however its role as a positive regulator of the E3 ligase Nrdp1 supports a model whereby, loss of Clec16a leads to accumulation of the Nrdp1 substrate and mitophagy regulator Parkin. Interestingly, elevated Parkin causes increased early-mitophagy which when coupled with impaired autophagosomal trafficking in late mitophagy results in accumulation of defective mitochondria as well as the associated negative effects in β-cell function (102).

Like most secretory cells, β-cells are sensitive to ER-stress. The ubiquitin-like protein UFM1 and its interacting partners UFBP1, CDK5AP3, and the E3 ligase UFL1 are highly enriched in pancreatic islets and are induced in the presence of ER-stress (105). Silencing the E3 ligase UFL1 enhances ER-stress induced apoptosis in β-cells. Collectively, these data emphasize the importance of the UPS in β-cell biology and provide specific examples where E3 ligases affect β-cell function.

The Role of PJA2 in Insulin Secretion

PJA2 (also known as PRAJA2 or Neurodap1) is a 78 kDa protein shown to have E2-dependent E3 ligase activity(106). Not much is known about the role of PJA2 in β-cells however, it has quickly emerged as an important regulator of key signaling pathways. It has been implicated as an A-kinase anchor protein (AKAP) that binds the regulatory subunits of PKA (107). Furthermore, PKA phosphorylation of PJA2 at two residues promotes subsequent ubiquitination and degradation of PKA regulatory subunits. Loss of regulatory subunits has been shown to contribute to enhanced cAMP signaling which promotes long-term memory generation in neurons. In addition to regulating cAMP signaling, PJA2 has been shown to promote glioblastoma growth by ubiquitinating and degrading Mob1, a positive regulator of the tumor suppressor Hippo-pathway(108). And more recently, PJA2 has been shown to regulate calcium signaling in pancreatic β-cells and promote β-cell functional compensation (65). Due to the emerging importance of PJA2 in several key pathways, it has become worthwhile to explore the mechanism of PJA2 regulation. PJA2, like many E3 ligases, appears to undergo auto-ubiquitination to regulate its own levels (unpublished data; Screaton Lab). To prevent E3 ligase levels from decreasing too drastically

and thus negatively affecting its function in ubiquitinating substrates, E3 ligases have developed several key methods to protect against overt auto-ubiquitination. In particular, E3 ligases can (a) interact with complex partners or (b) substrates to prevent auto-ubiquitination. In addition, E3 ligases can undergo (c) post-translational modifications which protect against auto-ubiquitination or (d) interact with de-ubiquitinating enzymes (109). It is unclear if PJA2 has complex partners that protect the E3 ligase from auto-ubiquitination or whether PJA2 substrates or de-ubiquitinating enzymes modulate PJA2 auto-ubiquitination.

It has been shown that the E3 ligase Mdm2 and its homologue MdmX are able to undergo auto-ubiquitination and this is enhanced when the two E3 ligases are present together (110). However, the synergistic effect of Mdm2 / MdmX ubiquitination does not increase p53 substrate ubiquitination. Interestingly, E3 ligase auto-ubiquitination can be an activating event. Contrary to the previous findings, a recent study by Ranaweera and Yang demonstrated that Mdm2 auto-ubiquitination facilitates enhanced p53 polyubiquitination (111). Furthermore, this effect was lost when the ubiquitin-binding domain (UBD) on E2 ubiquitin-conjugating enzyme was mutated. The authors reasoned that Mdm2 auto-ubiquitination allowed for greater recruitment of E2 via interaction between polyubiquitin chains on Mdm2 and the UBD of the E2. It stands to reason that an enhanced recruitment of E2 enzyme will result in increased processing of substrate ubiquitination. Given this pretext, PJA2 auto-ubiquitination could simply be a mechanism of auto-regulation or it could be contributing to enhanced p35 polyubiquitination.

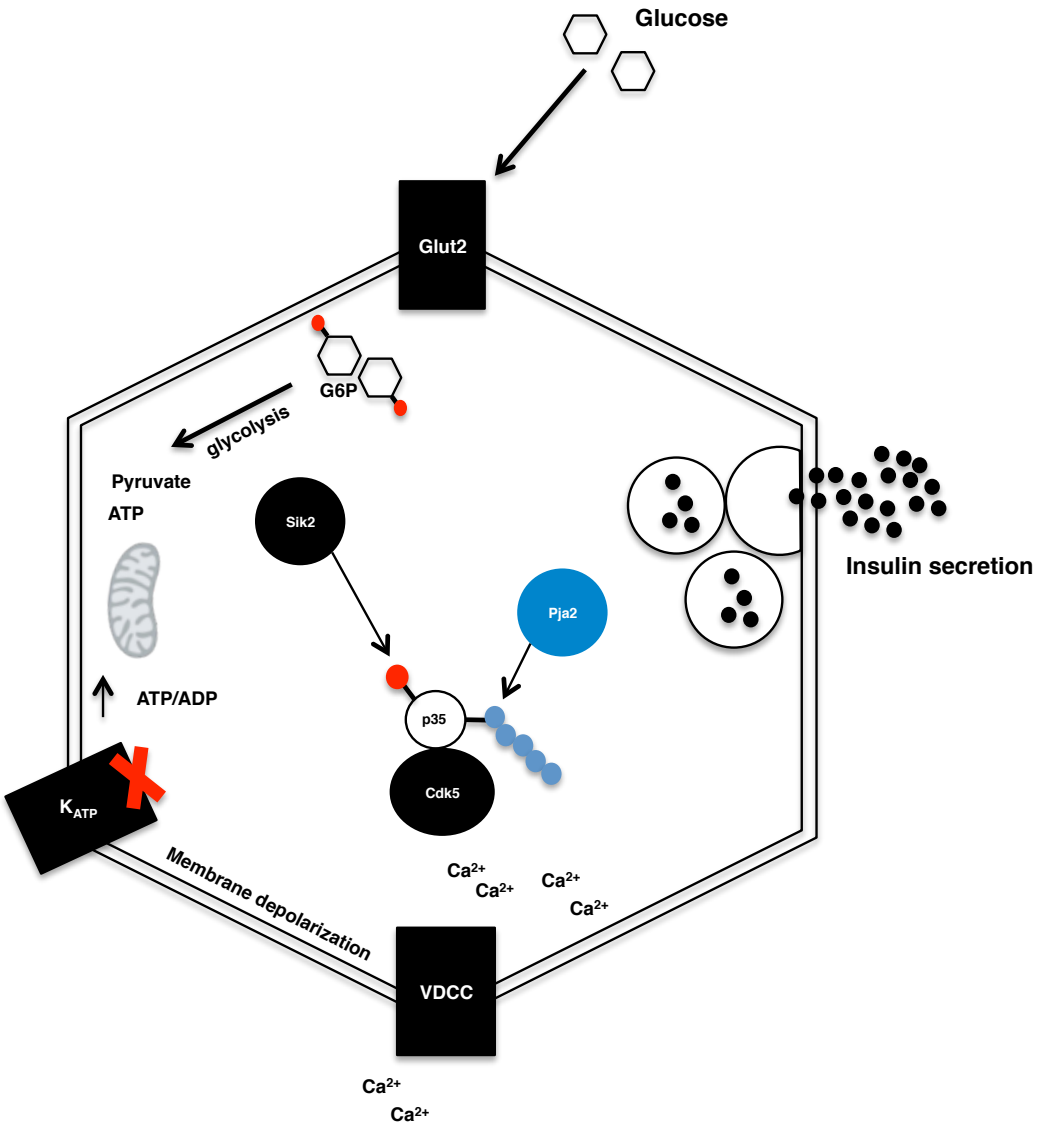
Glucose
Glut2
G6P
glycolysis
Pyruvate
ATP
Sik2
Pja2
Insulin secretion
ATP/ADP
p35
Cdk5
K ATP
Membrane depolarization
Ca2+
Ca2+
Ca2+
Ca2+
VDCC
Ca2+
Ca2+

Figure I: Classical model of insulin secretion juxtaposed with newly elucidated SIK2-p35-PJA2 pathway. In the classical model of insulin secretion, pancreatic β-cells in the islets of Langerhans sense extracellular glucose and utilize the GLUT2 glucose transporter to shuttle glucose into the cell. Following, glucose is phosphorylated by glucokinase and undergoes glycolysis to generate ATP and pyruvate, which can undergo further processing to generate more ATP. Increased ATP/ADP ratio in the beta cell leads to K_{ATP} channel closure, membrane depolarization, calcium ion influx through voltage-dependent calcium channels (VDCC) and subsequent insulin secretion. P35-CDK5 complex phosphorylates Ser783 of the VDCC and attenuates calcium influx and consequently reduces insulin secretion. SIK2 phosphorylation of p35 at Ser91 followed by PJA2-mediated ubiquitination and degradation results in reduced p35 levels and CDK5 activity and elevated insulin secretion.

RNAi Screening Technology

Genetic screening is an invaluable tool in unraveling the complexity of cell biology. With approximately 30,000 human genes, the need for screening becomes evident in finding associations between genetic function and disease states. In the case of diabetes, the goal is to identify genes that regulate β-cell function. In particular, characterizing genes that regulate insulin secretion can lead to novel diabetes therapy. The ultimate goal of characterizing candidates from genetic screens is to couple the genetic findings with small molecule chemical screening. Burns et al. developed an exciting new high-throughput luminescent reporter of insulin secretion (112). By inserting Gaussia lucerifase into the c-peptide region of pro-insulin, β-cells demonstrate reliable co-secretion of insulin and lucerifase. This allows for precise measurement of insulin secretion through the luciferase proxy. Furthermore, this approach provides the advantage of being cost-effective due to its non-reliance on ELISA. In fact, Burn and colleagues validate their system by performing a 1600 compound screen and ultimately identify negative and positive regulators of glucose-stimulated insulin secretion.

Hypothesis

Our lab and others have demonstrated that the p35/CDK5 pathway is important for insulin secretion. Furthermore, phosphorylation of p35 at Ser91 by the AMPK family member SIK2 promotes p35 ubiquitination and degradation by the RING E3 ligase PJA2. We hypothesize that PJA2 undergoes auto-ubiquitination. Furthermore, we hypothesize that p35 levels can be modulated by regulating PJA2 stability. In particular, a stabilized PJA2

mutant (K3R) is able to regulate endogenous p35 levels and could therefore be therapeutically beneficial for promoting β-cell function.

Research Objectives

1. **Identify novel regulators of insulin secretion by using RNAi to knockdown p35 interactor genes. Characterize the mechanism of p35 regulation.**
2. **Characterize PJA2 auto-regulation by identifying auto-ubiquitination sites. Use site-directed mutagenesis to generate stable PJA2 mutants and compare function to wild-type PJA2.**
3. **Find signal dependent regulation of PJA2 in pancreatic β-cells and study the effect on functional output of insulin secretion.**

1. **Identify novel regulators of insulin secretion by using RNAi to knockdown p35 interactor genes.**

   Flag-CDK5R1 (p35) was used in an affinity purification coupled with mass spectrometry (AP-MS) to identify proteins interacting with p35 (65). A list of candidate genes potentially regulating p35 was generated. The objective was to use RNAi to knockdown these candidate p35-interactor genes and monitor p35 levels as a readout. Due to the large sample of genes, a high-throughput approach was used to generate lentivirus encoding shRNA. Three shRNA per gene were designed to ensure that at least 1 of the shRNA successfully knocked-down the gene of interest with minimal off-target effects. Secondly, the shRNA fragment was cloned into a green fluorescent protein-expressing vector (pLKO.1GFP) to ensure that virus production could be monitored. The virus was then aliquoted in a 96-well format to facilitate

high-throughput screening. Lastly, SDS-PAGE was employed to detect p35 levels after knockdown of individual genes. Genes that show changes in p35 levels after knockdown in at least 2 shRNA were followed up with more rigorous validation approaches.

2. **Characterize PJA2 auto-regulation by identifying auto-ubiquitination sites.**

   There is evidence to suggest that PJA2 undergoes auto-regulation (unpublished data; Screaton Lab). In particular, an E3-ligase defective ring mutant of PJA2 (C633A/C670A referred to as 2CA from here on) was able to stabilize PJA2 protein levels. In addition, MG132 treatment stabilizes PJA2 suggesting that the E3-ligase itself is regulated by the ubiquitin proteasome system. Given this pretext, I began with a literature search in combination with surveying post-translational modification databases (such as GGBase and Phosphosite) to identify known ubiquitination sites of PJA2. Following, I employed site-directed mutagenesis to generate lysine to arginine mutations of the predicted ubiquitination sites with the rationale that a K to R mutation would not undergo ubiquitination and therefore would stabilize PJA2. To test this, PJA2 lysine mutants were transfected in 293T HEK cells and PJA2 levels were monitored and compared with wild-type and 2CA mutant PJA2. Lastly, an in vitro ubiquitination assay was employed to test if the lysine mutant PJA2 was able to undergo auto-ubiquitination. Also, the ability of the mutant PJA2 to ubiquitinate and subsequently degrade its substrate, p35, was tested.

3. **Find signal dependent regulation of PJA2 in pancreatic β-cells and study the effect on functional output of insulin secretion.**

PKA is able to regulate PJA2 through phosphorylation at Ser339 and Thr385 (107). This phosphorylation is required for PJA2-mediated ubiquitination and subsequent degradation of regulatory subunits of PKA. I tested if PKA-mediated PJA2 activation was important for p35 turnover. First, I examined if PKA activation (through forskolin treatment) affected PJA2 auto-regulation. Afterwards, I tested to see if PKA activation affected p35 levels and more importantly, the functional output of insulin secretion in pancreatic β-cell models such as MIN6 cells. I also examined PJA2 self-interaction and whether this was regulated in a signal dependent manner. E3 ligases harboring RING domains often undergo self-interaction which can ultimately dictate the ligase activity (113). One hypothesis was that PJA2 can interact with itself to regulate its own levels or ligase activity. I performed immunoprecipitation experiments to demonstrate that PJA2 can co-ip with itself. To accomplish this, I co-transfected FLAG-tagged PJA2 and V5-tagged PJA2 and immunoprecipitated with anti-flag antibody. Furthermore, I examined if this self-interaction was cAMP-dependent by initially treating cells with the adenylyl cyclase activator forskolin.

Chapter 2: Materials and Methods

2.1 Tissue Culture

HEK 293T (passages 9-20) and MIN6 cells (passages 24-36) were cultured in high glucose (25 mM glucose) Dulbecco Modified Eagle Medium supplemented with 10% fetal calf serum, 1% penicillin, streptomycin. MIN6 medium was further supplemented with 100μM β-mercaptoethanol and filter-sterilized through a 0.22 μm pore filter. Both HEK 293T and MIN6 cells were cultured at 37°C with 5% CO_2.

Lentivirus encoding shRNA were prepared by transfecting HEK 293T (under passage 15) with pLKO.1 GFP and the lentiviral packaging vectors pCMV 8.74 and pMD2G using either polyethyleneimine (PEI) or Lipofectamine 2000 (Invitrogen) transfection reagents. Transfected cells (3.5 $x10^7$ or 1.5 $x10^7$ cells per 15 cm or 10 cm plate respectively) were incubated at 37°C /5% CO_2 for 72 hr followed by virus harvesting and concentration. In brief, media containing the virus was filtered-sterilized through a 0.22 μm pore filter, and supplemented with a 20% sucrose cushion followed by ultracentrifugation at 28, 000 g for 2 hr at 4°C. The virus pellet was resuspended in non-supplemented DMEM and aliquoted for storage at -80°C. A similar protocol was employed for generating lentiviral overexpression constructs. In brief, cDNA encoding PJA2 was cloned into pDONR 221 vector (Invitrogen) followed by gateway recombination into pLenti6 V5 /pLenti6.3-V5 expression vectors and subsequent virus production.

2.2 Western blotting

Cell were lysed with SDS (sodium dodecyl sulfate) sample buffer (50mM Tri-HCl pH 6.8, 10% Glycerol, 2% SDS, 0.5% bromophenol blue) supplemented with 20 mM DTT and boiled at 95°C for 5-10 min as previously described (78) . Briefly, lysates underwent SDS-PAGE on 6-12% SDS polyacrylamide gel at 150 V for 1 hr in Running Buffer (25 mM Tris Base, 192 mM Glycine, 0.1% SDS). Following, proteins were transferred onto a 0.45 μm PVDF membrane for 80 min at 100V in Transfer Buffer (25 mM Tris, 192 mM Glycine, 20% methanol). Afterwards, the PVDF membrane was blocked with 5% skim milk in 1X TBST for 30-60 min and incubated with primary antibody overnight at 4°C. Membranes were washed 15-60 min with 1X TBST before incubation with horseradish peroxidase linked secondary antibody (1:5000) in 5% milk. Membranes were washed 15-60 min before visualizing proteins with Amersham ECL Regular or Prime (GE Healthcare).

2.3 High-throughput RNAi Screen

A list of 26 candidate p35-interactor genes were generated from immunoprecipitation of FLAG-CDK5R1 coupled with mass spectrometry. Each candidate gene was analyzed to generate 3 short hairpin RNA (shRNA) per gene for a total of 78 shRNA using SIGMA's Mission shRNA library and The RNAi Consortium (TRC) database. Oligos corresponding to the shRNA were annealed and ligated into the pLKO.1 GFP vector with the added benefit of testing transfection/infection efficiency by GFP. Large scale lentivirus was prepared as previously explained and arrayed into a 96-well mother plate followed by further arraying into 10 daughter plates. For large scale knockdown experiment, 6 x 10^4 MIN6 cells were added onto an arrayed virus plate and incubated at 37°C for 72 hr. Cells were lysed and protein levels of p35 were analyzed by western.

2.4 Glucose Stimulated Insulin Secretion (GSIS)

MIN6 cells were seeded at 1.2 x 10^5 cells in 48-well plates and incubated with shRNA corresponding to RPAP3, PJA2, and non-targeting control. After 72-120 hr, cells were washed twice and incubated with 1 mM glucose in Kreb's Ringer Buffer (KRB; 128 mM NaCl, 4.8 mM KCl, 1.2 mM KH_2PO_4, 1.2 mM $MgSO_4$, 2.5 mM $CaCl_2$, 5 mM $NaHCO_3$, 10 mM HEPES, and 0.1% BSA) for 30 min. Following, cells were incubated with either 1 mM glucose KRB (glucose starved) or 20 mM glucose KRB (stimulated) for 1 hr after which the medium was collected for insulin concentration analysis. For insulin content measurement, cells were treated with acid-ethanol overnight (4 °C) and subjected to 2 hr speed vacuum evaporation followed by resuspension in deionized, distilled H_2O at 65°C for 15 min. Insulin secretion and content levels were quantified using a homogenous time-resolved fluorescence assay kit (HTRF from Cisbio Assays). Samples for low glucose, high glucose, and insulin content were serially diluted to fall within an insulin standard range of 0-10 ng/mL. Samples were incubated with 2 monoclonal antibodies (Eu3+-Cryptate and XL665) for 2 hr at room temperature before reading the 384-well white-walled fluorescence plate using a Synergy2 Biotek plate-reader.

2.5 In vitro ubiquitination assay

An in vitro ubiquitination reaction was prepared in a mastermix format with the following components: 20 nM E1 (UBE1 Boston Biochem), 35 nM E2 (Ube2D2/UbcH5b Boston Biochem), and 20 ng of ubiquitin in 1X UBQ Buffer (50 mM Tris-HCl pH 7.4, 100 mM NaCl, 5 mM $MgCl_2$, 4 mM ATP, 1 mM DTT). The reaction mixture was added onto immunoprecipitated Flag-PJA2 on agarose beads and supplemented with either GST control

or GST-p35 before incubation at 37°C for 1 hr. The reaction was terminated with an equal volume of 2X SDS sample buffer and heated at 95°C for 10 min before separation by SDS-PAGE and western analysis. Polyubiquitinated p35 substrate was detected with anti-p35 (C64B10 Cell Signaling p35/p25). Anti-Ubiquitin (P4D1 Cell Signaling) was used to detect polyubiquitinated species.

2.6 Co-immunoprecipitation

HEK293 T cells were transfected with empty vector control, wild type, 2CA mutant, and K3R mutant 3X-FLAG PJA2 constructs for 24-48 hr and harvested for FLAG-immunoprecipitation. Cells were lysed washed twice with PBS before collecting in lysis buffer (20 mM Tris-HCl pH7.5, 150 mM NaCl, 1% Triton X-100, 5% Glycerol, 10 mM NaF, 1 mM PMSF, 1X Protease Inhibitor Cocktail, 0.5 mM DTT). Lysates were pre-cleared for 2 hr with A/G agarose beads (Santa Cruz) before overnight incubation with primary anti-FLAG M2 (Sigma). Afterwards, 30 µl of the 50% slurry of A/G agarose beads was added to lysates and rotated at 4°C for 2 hr. Beads were thoroughly washed 3X with lysis buffer before addition of 2X SDS and boiling at 95°C for 5 min. Afterwards, lysates underwent SDS-PAGE and western blotting for detection of interacting partners.

2.7 Site-directed mutagenesis of Pja2 construct

Mutagenesis of PJA2 constructs was performed according to the Stratagene Quikchange™ Site-Directed Mutagenesis Kit. Briefly, forward and reverse primers harboring a single nucleotide mutation (to alter lysine residues into arginine) were designed according to manufacturer's guidelines. Next, a reaction mixture was set up on ice consisting of 1X Phusion GC Buffer, 200 mM dNTP, 0.5 µM forward and reverse primers, 50-250 ng

of template DNA, 3% DMSO, 1 unit of Phusion DNA Polymerase. The reaction was transferred to a thermocycler set to a standard PCR cycling condition (98°C for 10 sec, 35 cycles of [98°C for 10 sec, 55°C for 10 sec, 72°C for 30 sec/ kb], 72°C for 8 min, hold 4°C). Following, the PCR reaction was Dpn1 digested for 2-3 hr, transformed in STBL3 cells and plated on Ampicillin 100 μg/mL plates which were incubated at 30°C overnight. Afterwards, several clones were picked and grown at 30°C overnight to be mini-prepped and digest confirmed or sequenced to confirm presence of mutation.

2.8 Recombinant protein production

GST- p35, GST-p25, and GST-p10 were prepared as following. cDNA corresponding to p35, p25, or p10 was cloned into pGEX-6p-1 (GE Healthcare) bacterial expression vector using BamHI and XhoI restriction sites. The vectors were transformed in BL21 DE3 expression bacteria and an overnight starter culture was grown at 37°C. Starter cultures were diluted 25X in pre-warmed LB+ 100 μg/mL ampicillin and allowed to grow at 37°C until an OD_{600} of 0.6-0.8, followed by the addition of IPTG (0.2 mM) and 4 hr additional growth at 30 or 37°C. Next, cultures were spun down, washed with PBS, and lysed in lysis buffer (50 mM Tris pH 8.0, 200 mM NaCl, 1 mM, 1mM EDTA, 1 mM DTT, 1% TX-100, 1X protease inhibitor cocktail). Cells were sonicated at 12% Amp in 5 sec bursts until lysates appeared dark. Afterwards, samples were spun at 13,000g/ 4°C for 10 min and supernatant was transferred to new tube supplemented with pre-rinsed glutathione sepharose 4B beads (GE Healthcare). GST recombinant protein purification was done according to manufacturer's guidelines and eluted proteins were stored at -80°C.

Chapter 3: Results

3.1 Co-immunoprecipitation-coupled mass spectrometry identifies p35 interacting genes:

CDK5R1 has previously been linked to insulin secretion in pancreatic β-cells. It stands to reason that identifying upstream regulators of p35 levels can further elucidate this signaling pathway and generate other potential targets for insulin secretion defects. With this rationale, co-immunoprecipitation-coupled mass spectrometry was employed to identify proteins interacting with p35 **(Figure 1A, Appendix A&B)**. The candidate list of p35 interacting genes was highly promising because it identified CDK5, the canonical binding partner of p35. In addition, it identified other CDK family members such as CDK2, which have been shown to interact with p35. Interestingly, the list of p35 interacting proteins showed an abundance of E3 ligases or components of the E3 complex as well as the entire AMPK complex. To validate these intriguing potential interacting partners of p35, RNA interference was employed to examine if genetic knockdown of the identified genes would regulate p35 levels in the mouse pancreatic beta cell model MIN6 cell. Briefly, shRNA were generated and arrayed in 96-well plate and then MIN6 cells were reverse transfected for 72hr. Following, cells were harvested and proteins separated by SDS-PAGE and analyzed by western **(Figure 1B)**.

3.2 High-throughput screen identifies RPAP3 as regulator of p35 levels but not insulin secretion:

Knockdown of RPAP3 with two independent shRNA resulted in p35 elevation relative to non-target shRNA control **(Figure 2A)**. Furthermore, p35 elevation was comparable to the elevation seen by knocking down PJA2, the E3 ligase responsible for ubiquitination and degradation of p35.

A.

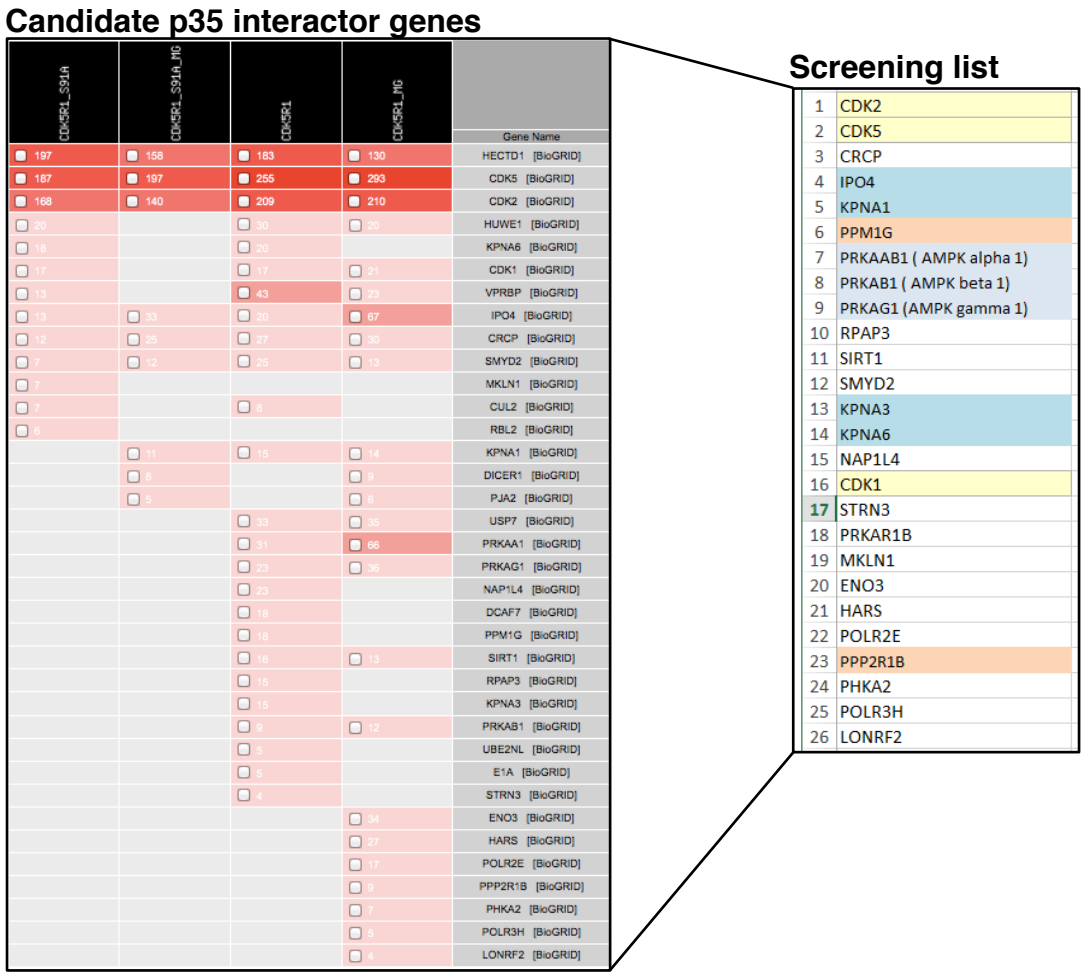

B.

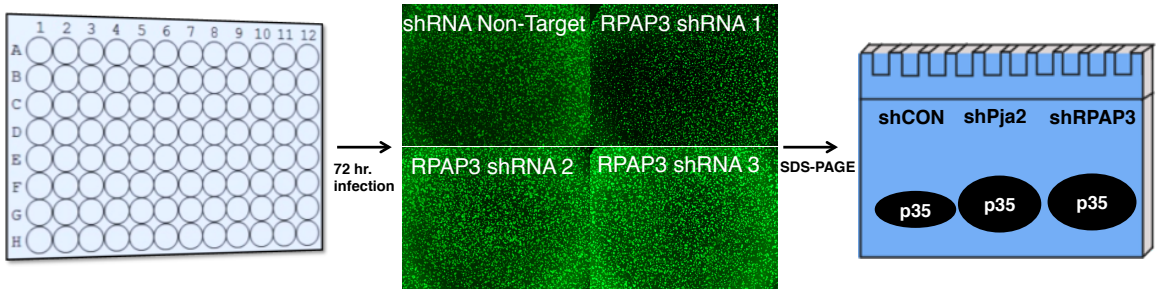

1. **Prepare 3 shRNA targeting interactor genes**
2. **Infect murine pancreatic beta cell line (Min6 cells) for 72hr.**
3. **Measure p35 levels by western blot as readout**

Figure 1. Outline of High-Throughput RNAi screen for candidate p35 interacting genes. (A) Cells expressing FLAG-CDK5R1 (or mutant) were treated with MG132 or DMSO control followed by immunoprecipitation with anti-FLAG antibody and coupled with mass spectrometry to identify p35-interacting proteins. Right: shortened gene list used for the high-throughput screen. **(B)** Outline of high-throughput screening protocol. For greater detail, refer to the materials and methods section of this thesis.

To further validate RPAP3 as a regulator of p35 levels, the functional consequence of RPAP3 knockdown in β-cells was addressed. Previous results showed that an increased p35 level in β-cells is associated with reduced insulin secretion. To address this, RPAP3 was knocked down in MIN6 cells and the functional output of insulin secretion was assayed. Knockdown of RPAP3 resulted in elevated p35 levels as shown previously, however compared to a non-targeting shRNA, RPAP3 knockdown did not significantly affect insulin secretion **(Figure 2C)**. Furthermore, overexpression of RPAP3 did not change p35 levels or insulin secretion **(Figure 2D)**. The purpose of identifying and characterizing p35 interacting partners was to study the functional output of insulin secretion in β-cells. With this guiding objective, it was not worthwhile to continue pursuing RPAP3 due to its lack of effect on insulin secretion. One plausible interpretation takes into account RPAP3's reported role as a chaperone protein **(Figure 2B)**. Knockdown of RPAP3 and subsequent loss of its chaperone functions is most likely associated with multiple biological consequences only one of which is p35 elevation. For this reason, global loss of RPAP3 function could theoretically result in p35 elevation without demonstrating the expected functional consequence of reduced insulin secretion. In light of this, the focus was shifted to characterizing PJA2 regulation of p35 and its role in insulin secretion.

3.3 PJA2 knockdown causes elevated p35 levels and reduced insulin secretion in MIN6 cells:

The E3 ligase PJA2 was among the genes identified to be interacting with p35. Furthermore, knockdown of PJA2 in pancreatic β-cells resulted in elevated p35 levels (**Figure 3A)**. More importantly, PJA2 knockdown was associated with reduced GSIS **(Figure 3B)**

A.

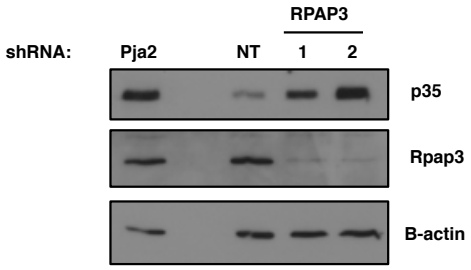
RPAP3
shRNA:
Pja2
NT
1
2
p35
Rpap3
B-actin

B.

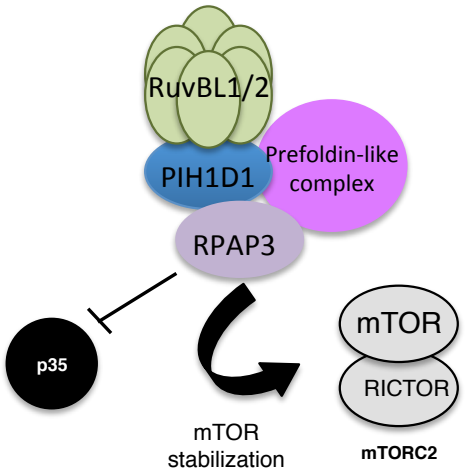
RuvBL1/2
PIH1D1
Prefoldin-like complex
RPAP3
p35
mTOR
RICTOR
mTOR stabilization
mTORC2

C.

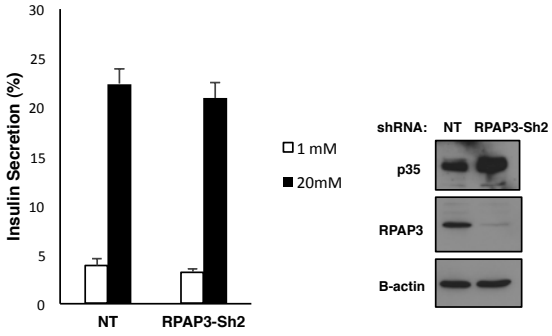
Insulin Secretion (%)
30
25
20
15
10
5
0
NT
RPAP3-Sh2
1 mM
20mM
shRNA:
NT
RPAP3-Sh2
p35
RPAP3
B-actin

D.

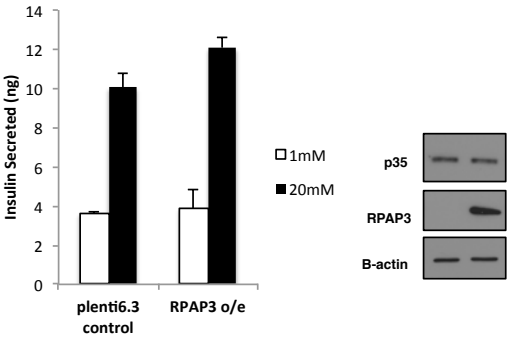
Insulin Secreted (ng)
14
12
10
8
6
4
2
0
plenti6.3 control
RPAP3 o/e
1mM
20mM
p35
RPAP3
B-actin

Figure 2: Validating RPAP3 as novel regulator of p35 levels and testing functional output of insulin secretion (A) Western blot showing p35 and RPAP3 levels after 72 hr knockdown of RPAP3 and positive control PJA2 in MIN6 cells. **(B)** Model depicting known role of RPAP3 as component of the R2TP complex. **(C) & (D)** GSIS experiment with corresponding western blots showing effects of RPAP3 silencing **(C)** and overexpression **(D)** in MIN6 cells.

A.

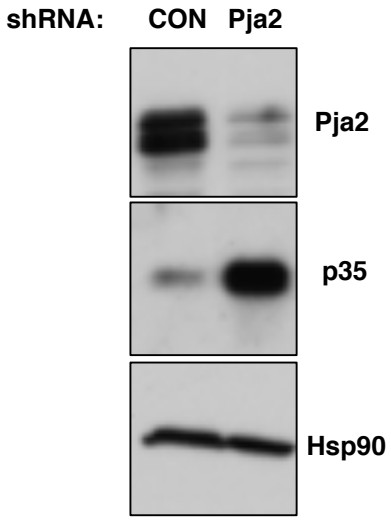
shRNA:
CON
Pja2
Pja2
p35
Hsp90

B.

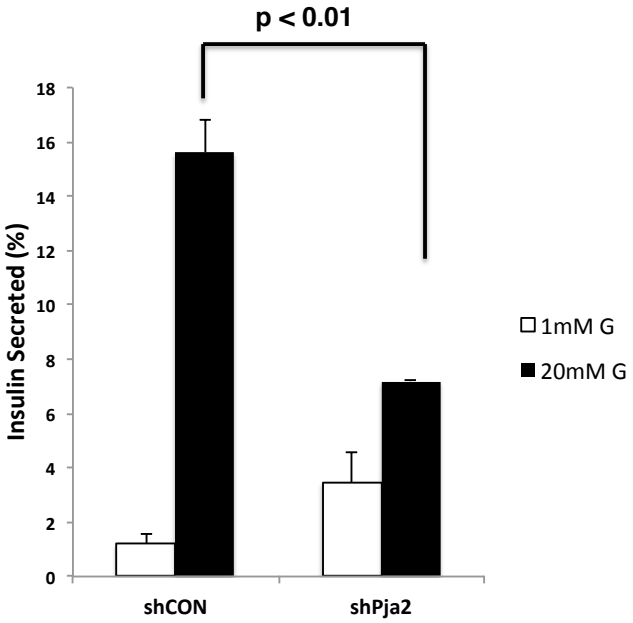
p < 0.01
Insulin Secreted (%)
18
16
14
12
10
8
6
4
2
0
shCON
shPja2
1mM G
20mM G

Figure 3. Knockdown of PJA2 in MIN6 cells causes increased p35 levels and reduced insulin secretion. (A) MIN6 cells were infected for 96 hr with lentivirus encoding either control shRNA or shPJA2. Cells were harvested and PJA2 knockdown was assessed through western. HSP90 was used as loading control. **(B)** MIN6 cells were infected for 96 hr with control shRNA or shPJA2 and harvested for GSIS assay. Insulin secretion was normalized to total insulin content.

3.4 PJA2 auto-regulates levels through auto-ubiquitination

E3 ligases are essential components of the ubiquitin proteasome system tasked with the role of targeting specific substrates with poly-ubiquitin chains and ultimately dictating the substrate's degradation. Interestingly, E3 ligases can self-regulate through a process termed auto-ubiquitination whereby the E3 ligase behaves as its own substrate. PJA2 is stabilized by the proteasomal inhibitor MG132, suggesting that the E3 ligase itself is regulated by the ubiquitin-proteasome system **(Figure 4B)**. An in vitro auto-ubiquitination assay demonstrated that wild-type PJA2 but not a catalytically inactive ring mutant is able to undergo auto-ubiquitination **(Figure 4A, 4C)**. In addition, β-cell specific PJA2 transgenic mice are unable to overexpress PJA2 **(data not shown).** Collectively, these observations support the model that PJA2 stability is dependent on the ubiquitin-proteasome system as well as an intact RING domain and more specifically that PJA2 undergoes auto-ubiquitination **(Figure 4D)**. Given that loss of PJA2 is associated with reduced insulin secretion, the next logical step was to address if the opposite were true. Namely, could PJA2 overexpression in pancreatic β-cells promote enhanced insulin secretion? Before this could be tested, it was imperative to overcome PJA2's propensity to auto-regulate levels through auto-ubiquitination.

3.5 Mutating lysine residues K317, K336, and K666 has no effect on PJA2 stability

With the narrative that PJA2 overexpression can potentially enhance insulin secretion coupled with data supporting a model that PJA2 undergoes auto-ubiquitination, it was necessary to establish a means to stabilize PJA2 levels. A bioinformatics approach was used to survey post-translational modification databases such as GGBase and PhosphositePlus® to identify potential auto-ubiquitination sites.

A

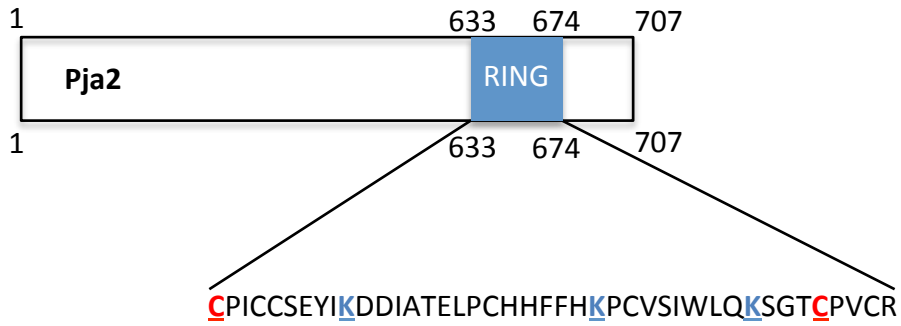
1
633
674
707
Pja2
RING
1
633
674
707
CPICCSEYIKDDIATELPCHHFFHKPCVSIWLQKSGTCPVCR

B.

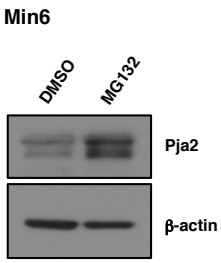
Min6
DMSO
MG132
Pja2
β-actin

C.

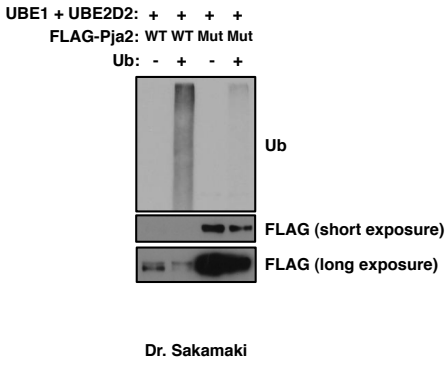
UBE1 + UBE2D2: + + + +
FLAG-Pja2: WT WT Mut Mut
Ub: - + - +
Ub
FLAG (short exposure)
FLAG (long exposure)
Dr. Sakamaki

D.

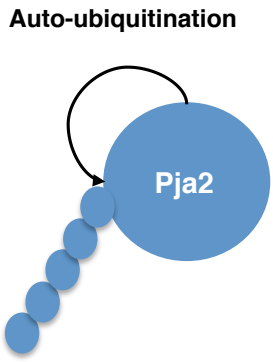
Auto-ubiquitination
Pja2

Figure 4. Pja2 auto-regulates protein levels through auto-ubiquitination. (A) Schematic representation of PJA2 RING domain amino acid sequence. Cysteines highlighted in red are necessary for E3 ligase enzymatic activity and mutated in the 2CA catalytically inactive mutant. **(B)** MIN6 cells were treated with the proteasomal inhibitor MG132 or DMSO control and cells are harvested for protein analysis of endogenous PJA2. β-actin was used as a loading control. **(C)** In vitro auto-ubiquitination assay of either FLAG purified wild-type PJA2 or 2CA mutant (Mut) in the presence of E1, E2, and Ub. Reaction was terminated with 2X SDS after 1 hr at 37°C before western analysis. **(C &D)** Unpublished data; Dr. Sakamaki **(D)** Schematic representation of PJA2 auto-ubiquitination.

The bioinformatics approach identified K317, K336, and K666 as lysine residues which have been reported to be post-translationaly modified by ubiquitination. Next, site-directed mutagenesis was used to generate lysine to arginine mutants with the rationale that these mutated residues will no longer undergo ubiquitination. To address the possibility that multiple lysine residues may be required for auto-ubiquitination, double mutants as wells a triple mutant were generated. Compared to wild-type PJA2, the catalytically inactive 2CA mutant was stabilized. However, mutations of lysine K317, K336, and K666 either individually or in combinations thereof showed no stabilization of PJA2 levels compared to the wild-type **(Figure 5B)**.

3.6 Mutating lysines K642, K657, and K666 in Ring Domain causes PJA2 stabilization and reduced auto-ubiquitination

The bioinformatics approach was further refined by incorporating post-translational modification prediction software. These software utilize algorithms generated from analyzing databases of experimentally reported ubiquitination sites. In addition, 3-dimensional prediction software was employed to generate a 3D protein structure of PJA2 in an effort to characterize the RING domain and lysine residues proximal to the RING domain. Based on these resources, several lysine to arginine mutants were generated and tested for stability. Among these was a RING domain triple mutant of lysines K642, K657, and K666 hereafter referred to as K3R. Compared to wild-type PJA2, the K3R mutant PJA2 was significantly stabilized when overexpressed in HEK 293T cells **(Figure 6A)**. The degree of stabilization observed with the K3R mutant was comparable to that of the 2CA mutant. As expected, cycloheximide experiments demonstrate that wild-type PJA2 undergoes rapid degradation **(Figure 6B)**. However, both K3R mutant as well as the 2CA control were stable

over time. Lastly, an in vitro auto ubiquitination assay showed that the K3R mutant has a significantly reduced ubiquitination signal compared to the wild-type **(Figure 6C)**. Interestingly, compared to the 2CA control, K3R mutant still demonstrates some auto-ubiquitination capacity.

A.

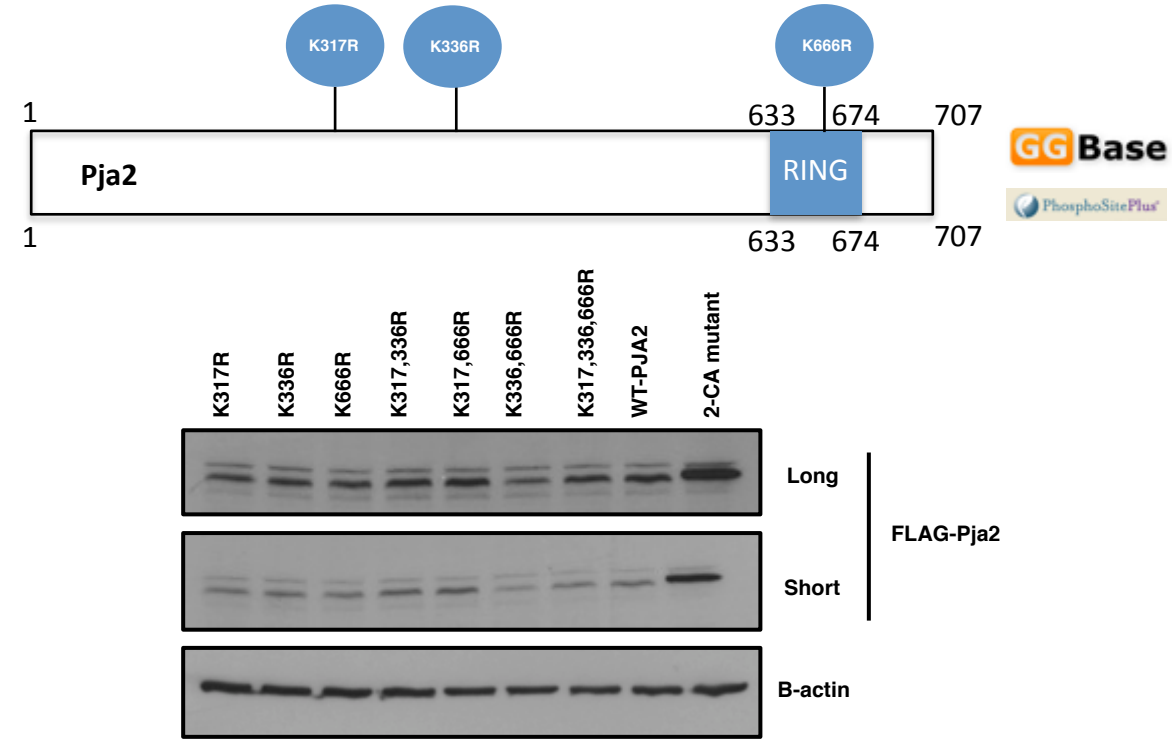
K317R
K336R
K666R
1
633
674
707
Pja2
RING
1
633
674
707
GG Base
PhosphoSitePlus
K317R
K336R
K666R
K317,336R
K317,666R
K336,666R
K317,336,666R
WT-PJA2
2-CA mutant
Long
Short
FLAG-Pja2
B-actin

Figure 5. Mutating reported ubiquitination sites K317, K336, K666 to arginine has no effect on PJA2 stability. (A) Schematic representation of PJA2 lysines K317, K336, and K666 identified through bioinformatics search of post-translational modification databases GGBase and PhosphoSitePlus®. (**B)** HEK 293T cells were transfected for 48 hr with either FLAG-tagged wild-type PJA2, single, double or triple mutants. 2CA mutant was used as a positive control of PJA2 stability. B-actin is used as a loading control

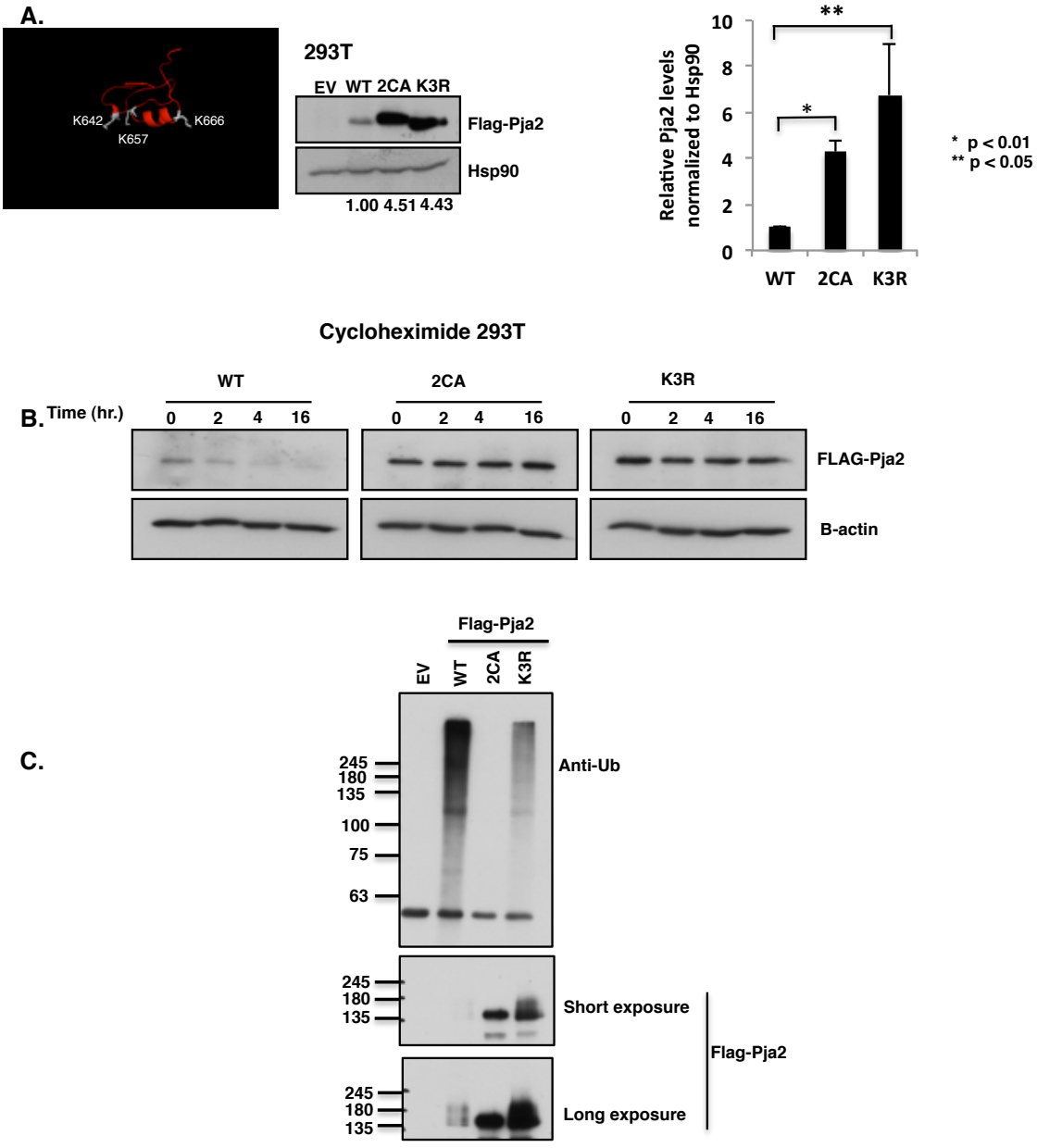
A.
K642
K657
K666
293T
EV WT 2CA K3R
Flag-Pja2
Hsp90
1.00 4.51 4.43
Relative Pja2 levels normalized to Hsp90
10
8
6
4
2
0
**
*
WT
2CA
K3R
* p < 0.01
** p < 0.05
Cycloheximide 293T
B.
Time (hr.)
WT
2CA
K3R
0 2 4 16
FLAG-Pja2
B-actin
C.
Flag-Pja2
EV
WT
2CA
K3R
245
180
135
100
75
63
Anti-Ub
Short exposure
Long exposure
Flag-Pja2

Figure 6. Mutating lysines K642, K657, K666 in the RING domain causes PJA2 stabilization and reduced auto-ubiquitination. (A) Schematic diagram depicting PJA2 RING domain. The 3 RING domain lysines K642, K657, and K666 are highlighted in gray. HEK 293T cells were transfected with either wild-type, 2CA-mutant, or K3R mutant PJA2 or empty vector control for 48 hr before cells were harvested for protein analysis. HSP90 was used as a loading control. PJA2 levels from 3 independent experiments were quantified and plotted on the right. **(B)** HEK 293T cells were transfected with wild-type PJA2, 2CA or K3R mutants. After 48 hr, cells were treated with 10 μg/ml cycloheximide for the indicated times before harvesting for protein analysis. B-actin was used as a loading control. **(C)** FLAG-PJA2 (wild-type, 2CA, or K3R mutant) was purified from HEK 293T cells. Following, an in vitro auto-ubiquitination assay was performed by supplementing with E1, E2 (Ube2D2) ligases and the reaction was subsequently terminated with an equal volume of 2X SDS after 1 hr at 37°C. PJA2 auto-ubiquitination was assessed by western analysis.

3.7 PJA2 Ring domain mutant K3R is functional with reduced activity compared to wild-type PJA2

Certainly, the K3R mutant demonstrates enhanced stability compared to wild-type PJA2 suggesting a reduced capacity to undergo auto-ubiquitination. Given that the K3R mutations are situated in the RING domain of PJA2, the next logical step was to address the source of the stabilizing effect. Namely, does the K3R mutant stabilize because tampering with lysine residues in the RING domain impairs enzymatic activity or does the stability arise due to loss of the auto-ubiquitination sites? To address this, in vitro ubiquitination assays were employed comparing the enzymatic activity of wild-type and mutant PJA2 against GST-tagged p35 substrate. Firstly, both wild-type and K3R mutant but not the catalytically defective 2CA mutant were able to polyubiquitinate GST-p35 **(Figure 7A).** The reaction was carried out in 4°C to rule out the possibility that GST-p35 was modified prior to the reaction. Secondly, comparing wild-type and K3R Pja2 between the control 4°C condition and the 37°C reaction demonstrates that wild-type PJA2 levels decrease while K3R mutant levels remain stable. Collectively, these data support the model that K3R mutant undergoes reduced auto-ubiquitination but unlike the 2CA mutant is able to maintain enzymatic activity and the capacity to ubiquitinate its substrate.

In addition to verifying if the enzymatic activity of the K3R mutant was intact, it was worthwhile to address the relative enzymatic activity of the K3R mutant compared to wild-type PJA2. An in vitro ubiquitination time-course experiment demonstrated that both wild-type and K3R mutant were able to ubiquitinate GST-p35. However, the rate of ubiquitination appeared greater with the wild-type PJA2 compared to K3R **(Figure 7B & 7C, Appendix F)**.

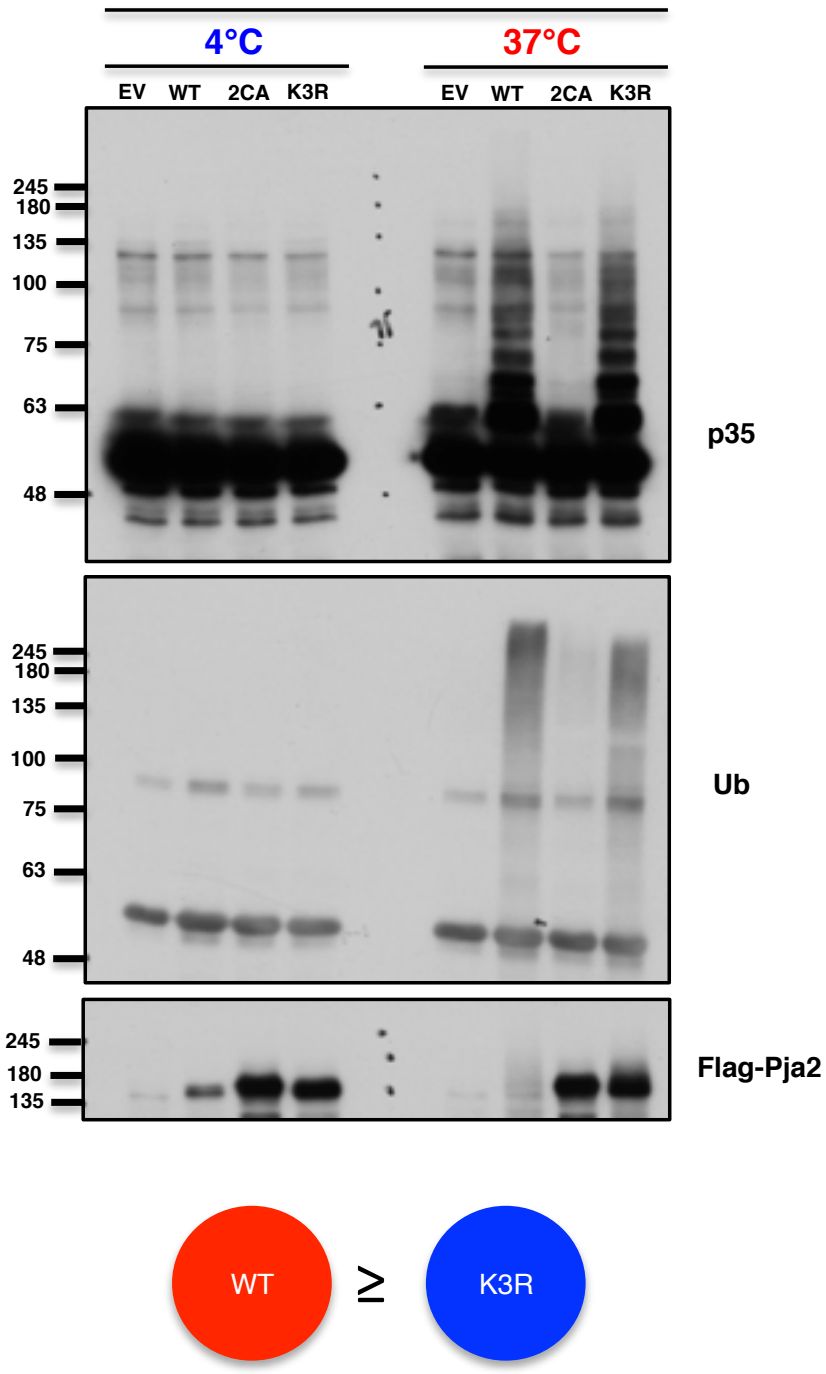
GST-p35
4°C
37°C
EV WT 2CA K3R
EV WT 2CA K3R
245
180
135
100
75
63
48
p35
Ub
Flag-Pja2
WT
≥
K3R

Figure 7a. PJA2 K3R mutant is functional and demonstrates E3 ligase enzymatic activity. In vitro ubiquitination assay with empty vector (EV), wild-type PJA2, 2CA and K3R mutants supplemented with GST-p35 substrate. The reaction was run at 37°C and 4°C control. Reactions were terminated with 2X SDS and separated by SDS-PAGE before blotting for p35, and Ub.

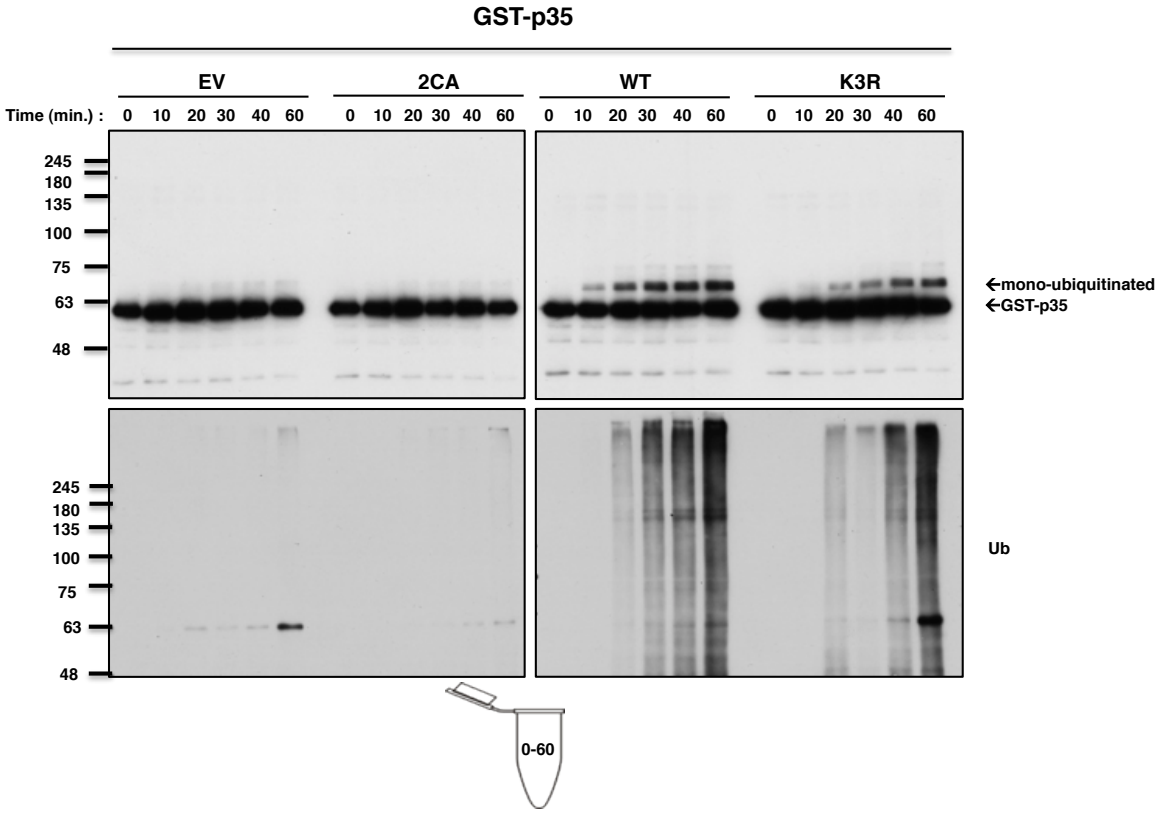
GST-p35
EV
2CA
WT
K3R
Time (min.) :
0 10 20 30 40 60
245
180
135
100
75
63
48
←mono-ubiquitinated
←GST-p35
Ub
0-60

Figure 7b. PJA2 K3R mutant is functional and demonstrates E3 ligase enzymatic activity. In vitro ubiquitination time-course assay testing wild-type PJA2, 2CA and K3R mutant ability to ubiquitinate GST-p35 substrate. Samples were incubated at 37°C and aliquots were removed after each time point and mixed with equal volume of 2X SDS before separation by SDS-PAGE and subsequent blotting for p35 and ubiquitin.

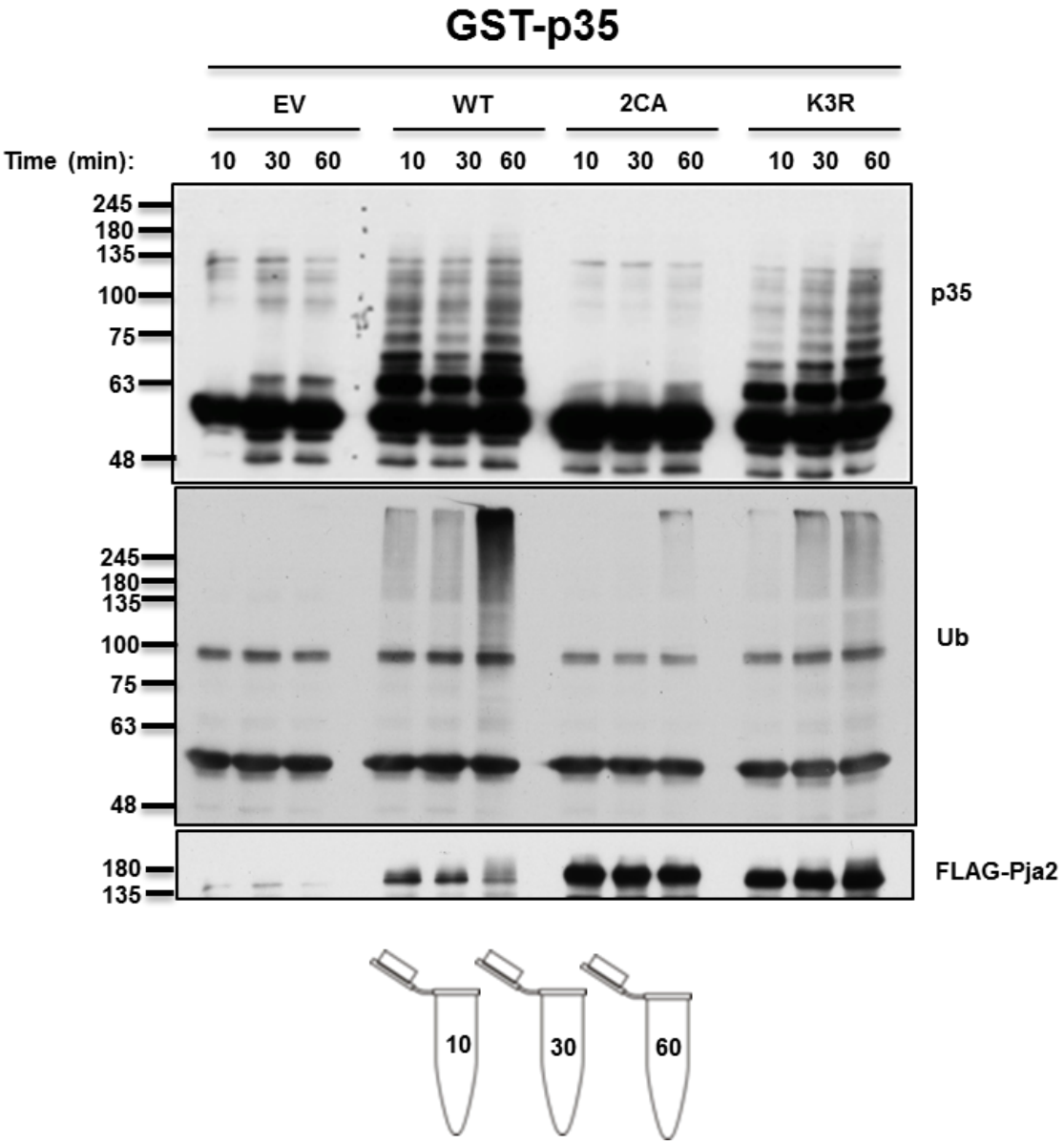
GST-p35
EV
WT
2CA
K3R
Time (min):
10 30 60 10 30 60 10 30 60 10 30 60
245
180
135
100
75
63
48
p35
245
180
135
100
75
63
48
Ub
180
135
FLAG-Pja2
10
30
60

Figure 7c. PJA2 K3R mutant is functional and demonstrates E3 ligase enzymatic activity. In vitro ubiquitination time-course assay testing wild-type PJA2, 2CA and K3R mutant ability to ubiquitinate GST-p35 substrate. Samples were incubated at 37°C in separate reaction tubes before stopping the reaction with an equal volume of 2X SDS. Lysates were separated by SDS-PAGE followed by blotting for p35 and ubiquitin.

3.8 PJA2 overexpression in MIN6 cells shows high infection rate for 2CA and K3R mutants

Indeed wild-type PJA2 undergoes rapid degradation through a mechanism of auto-ubiquitination. Furthermore, the K3R mutant demonstrates enhanced stability compared to wild-type PJA2 and maintains enzymatic activity supporting the conclusion that its capacity to undergo auto-ubiquitination has been hampered. The next logical objective was to look at biological relevance of these findings. In precise terms, does overexpression of PJA2 (wild-type or K3R) promote enhanced p35 degradation? More importantly, does PJA2 overexpression have a functional effect on β-cell biology by promoting enhanced insulin secretion? To address these questions, MIN6 pancreatic β-cells were infected with lentivirus encoding either an empty vector (EV) control or constructs corresponding to FLAG-tagged wild-type PJA2, 2CA or K3R mutant. Immunofluorescence allowed for the assessment of degree of infection after 72 hr. As expected, the EV control shows a negligible FLAG signal whereas wild-type PJA2 as well as 2CA and K3R mutants demonstrate strong signals **(Figure 8)**. In addition, the FLAG-PJA2 signal appears to cover more cells in the 2CA and K3R conditions compared to the wild-type.

3.9 Overexpression of PJA2 does not significantly affect insulin secretion in Min6 cells

Next, the effect of PJA2 overexpression in mouse pancreatic β-cells was examined. As verified by western, overexpression of PJA2 constructs was successful compared to an empty vector control **(Figure 9A & 9B)**. Glucose-stimulated insulin secretion was only significantly increased in wild-type PJA2 despite similar levels of overexpression between wild type and K3R **(Figure 9A)**. Changing the glucose stimulus to a gradient format showed

significant elevation of insulin secretion in 2CA and K3R mutant at the 20 mM glucose concentration.

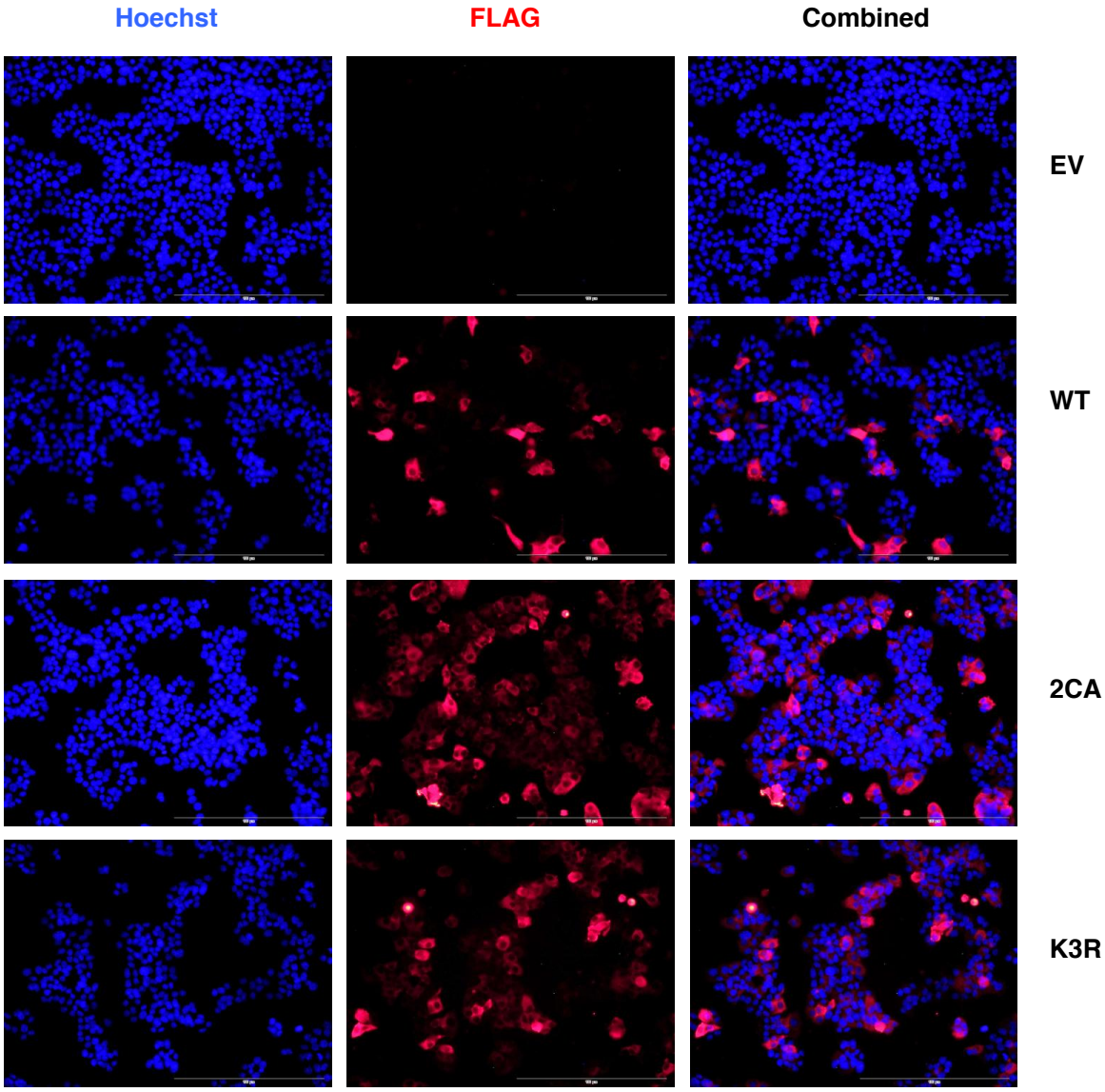

Figure 8. Immunofluorescence of MIN6 cells infected with lentivirus PJA2 overexpression constructs shows relatively high infection rate. MIN6 cells were infected for 72 hr with lentiviral constructs overexpressing wild-type PJA2, 2CA and K3R mutants and empty vector (EV) control. Cells were stained with Hoechst and anti-FLAG for DNA and FLAG-PJA2 respectively.

A.

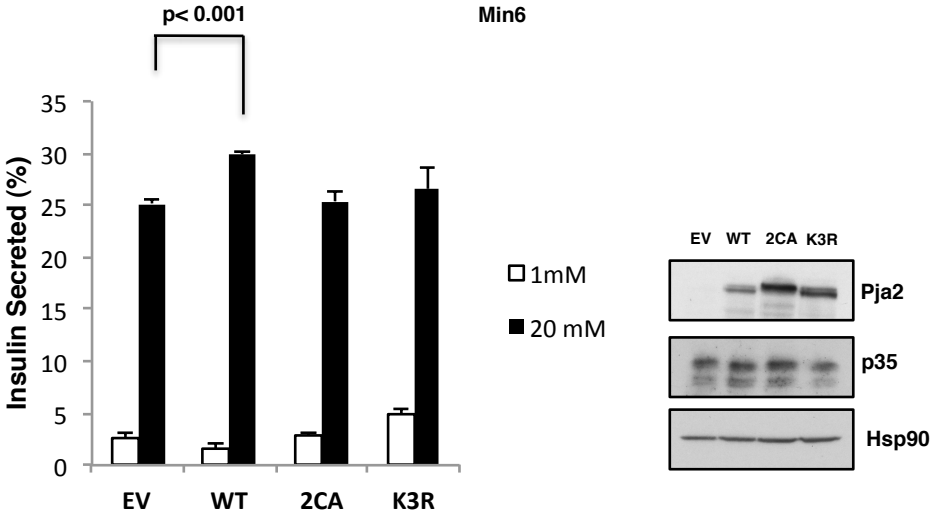

B.

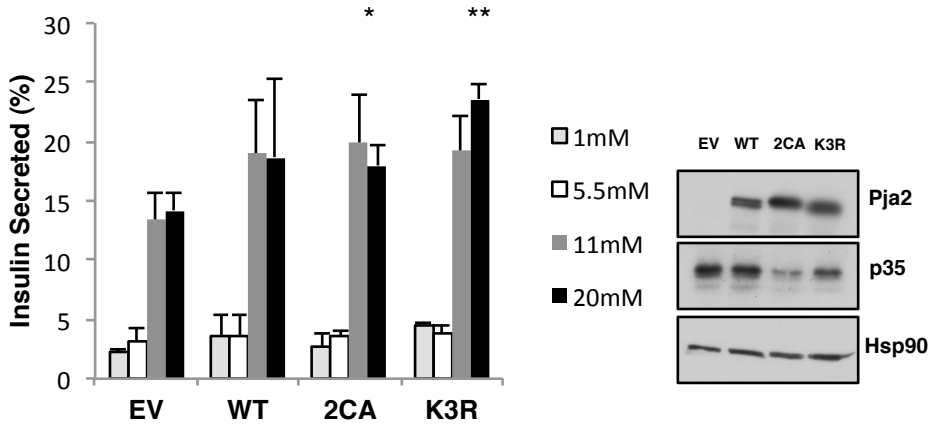

*p<0.05
**P <0.001

Figure 9. PJA2 overexpression in MIN6 cells shows weak correlation with insulin secretion. (A) MIN6 cells were infected for 72 hr followed by GSIS assay. PJA2 overexpression was assessed by western. **(B)** MIN6 cells were infected for 72 hr followed by a glucose titer GSIS assay. PJA2 overexpression was assessed by western. HSP90 was used as a loading control.

Of note, overexpression of K3R mutant but not wild-type PJA2 was significantly associated with decrease in endogenous p35 levels **(Appendix G)**.

It is evident that p35 levels are tightly regulated and thus do not fluctuate beyond a stable steady state. To test if overexpression of PJA2 can demonstrate robust regulation of endogenous p35, it was important to add an additional layer of p35 perturbation. More specifically, endogenous p35 levels needed to be elevated before PJA2 overexpression to test if p35 levels could be reduced dynamically. To accomplish this, shRNA targeting SIK2 was co-infected with PJA2 constructs with the rationale that SIK2 knockdown would result in elevated p35 level. Results showed no significant change in p35 levels after co-infecting shSIK2 and PJA2 constructs relative to an empty vector control **(Figure 10)**.

There is a possibility that PJA2 overexpression was not complete and that there exists a population of cells which were not infected. If this were the case, the population of uninfected cells would mask the true phenotype of PJA2 overexpression. One way to overcome this caveat is to overwhelm the cells with a large concentration of virus with the goal of increasing infection to near 100%. Doubling the volume of concentrated lentivirus of PJA2 constructs showed a significant reduction in insulin secretion **(Figure 11A)**. The combination of increased virus concentration and longer incubation time resulted in even a greater reduction in insulin secretion in wild-type, 2CA, and K3R. A variant of the 'hammer approach' was to use 'attenuated protein expression vectors'. The rationale was that by truncating the CMV promoter in the expression vector, protein expression could be fine tuned to overexpress at near endogenous levels. The benefit of this strategy was the ability to homogenously infect a large population of cells without overexpressing supra-endogenous levels **(Figure 12A)**.

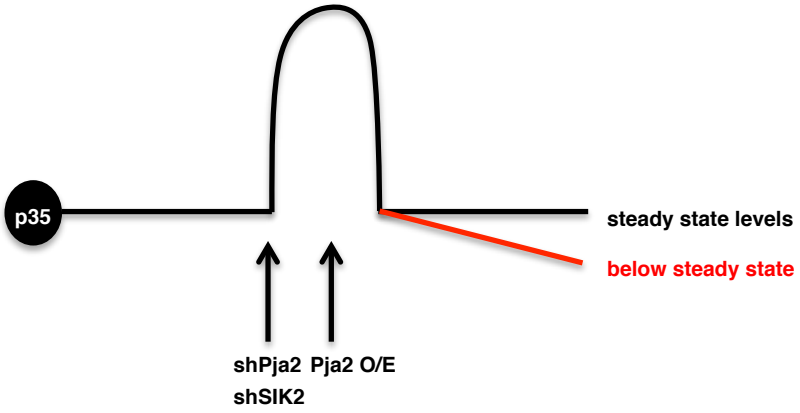
p35
steady state levels
below steady state
shPja2
shSIK2
Pja2 O/E

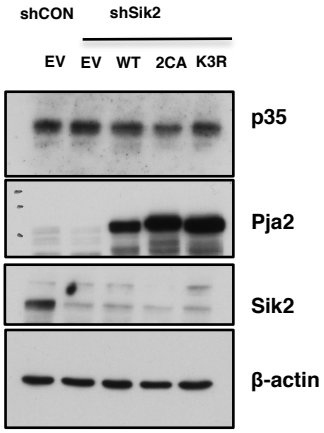
shCON
shSik2
EV
EV
WT
2CA
K3R
p35
Pja2
Sik2
β-actin

Figure 10. SIK2 knockdown coupled with PJA2 overexpression does not show p35 level regulation in MIN6 cells. MIN6 cells were infected with lentivirus encoding non-targeting shRNA or shRNA targeting SIK2 in the presence of PJA2 overexpression constructs or empty vector control. After 72hr infection, cells were lysed and harvested for western analysis. β-actin was used as a loading control.

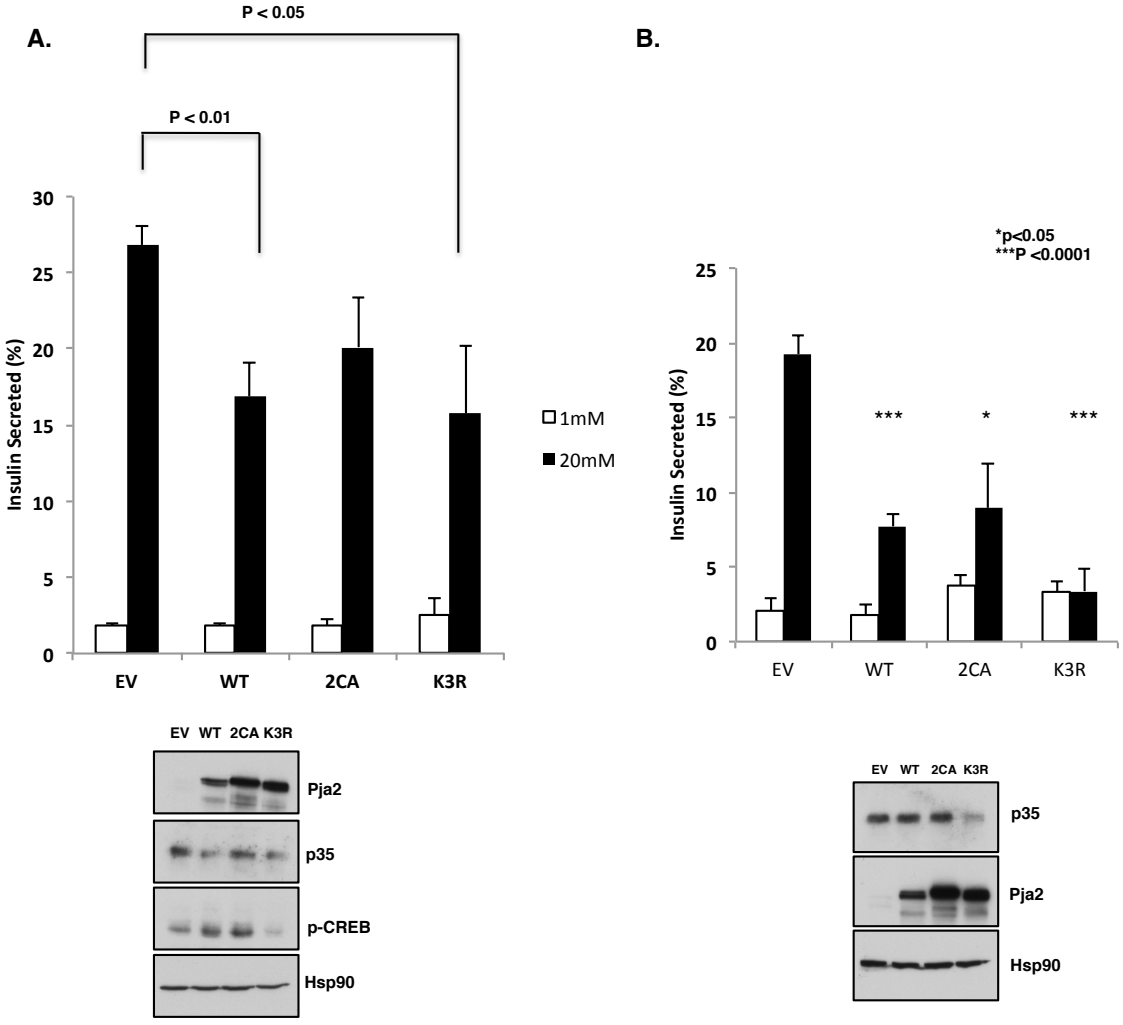
A.
P < 0.05
P < 0.01
Insulin Secreted (%)
30
25
20
15
10
5
0
EV
WT
2CA
K3R
1mM
20mM
EV WT 2CA K3R
Pja2
p35
p-CREB
Hsp90
B.
*p<0.05
***P <0.0001
Insulin Secreted (%)
25
20
15
10
5
0
***
*
***
EV
WT
2CA
K3R
EV WT 2CA K3R
p35
Pja2
Hsp90

Figure 11. Increased virus amount results in better p35 regulation but reduced insulin secretion after PJA2 overexpression in MIN6 cells. MIN6 cells were infected with 16 µl of concentrated lentivirus for 72 hr **(A)** or 96 hr **(B)** before harvesting cells for western and GSIS assays. HSP90 was used as a loading control.

A.

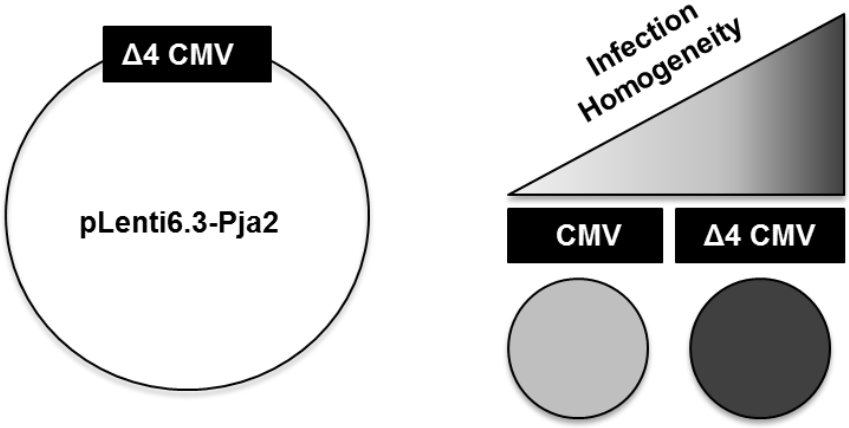
Δ4 CMV
pLenti6.3-Pja2
Infection Homogeneity
CMV
Δ4 CMV

B.

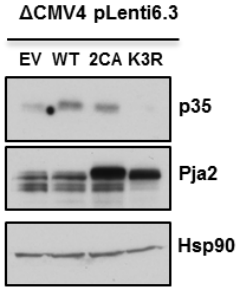
ΔCMV4 pLenti6.3
EV WT 2CA K3R
p35
Pja2
Hsp90

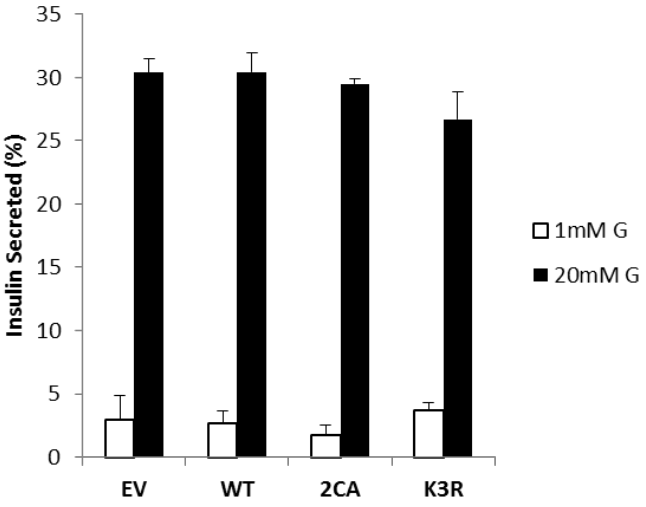
Insulin Secreted (%)
35
30
25
20
15
10
5
0
EV
WT
2CA
K3R
1mM G
20mM G

Figure 12. MIN6 cells infected with Δ4 CMV PJA2 constructs were able to express PJA2 near endogenous levels but did not affect insulin secretion. (A) Schematic diagram demonstrating Δ4 CMV plenti6.3 lentiviral expression vector and its enhanced capacity to express homogeneously. **(B)** MIN6 cells were infected with lentivirus encoding Δ4 CMV plenti6.3 PJA2 (wild-type or 2CA, K3R mutants) or empty vector control. After 72 hr, cells were harvested for protein analysis and GSIS assays. HSP90 was used as a loading control.

Overexpressing PJA2 constructs in the attenuated overexpression vector Δ4 CMV resulted in near endogenous expression of wild-type PJA2 with 2CA and K3R showing slightly increased levels **(Figure 12B)**. Interestingly, there was no significant change in GSIS with the use of attenuated expression vector.

3.10 PJA2 undergoes self-interaction, which is independent of cAMP signaling

E3 ligases often undergo auto-ubiquitination as a means of self-regulation. This process can be *cis* wherein an individual E3 ligase directly ubiquitinates itself. In addition, auto-ubiquitination can be *trans* mediated where multiple E3 ligases interact and ubiquitinate one another. To test this hypothesis, PJA2 was differentially tagged with FLAG and V5 and co-expressed in HEK 293T cells before performing co-immunoprecipitation. Interestingly, immunoprecipitation of FLAG-PJA2 results in co-ip with V5-PJA2 **(Figure 13A)**. Furthermore, this interaction was stabilized with the proteasomal inhibitor MG132. To further characterize this interaction, the effect of PJA2 phosphorylation was examined. Indeed, it has been reported that PKA phosphorylates PJA2 at residues S339 and T385. Before co-immunoprecipitation, cells were treated with the adenylyl cyclase activator forskolin or DMSO control with the rationale that forskolin treatment would increase intracellular cAMP and activate PKA. As a proxy for PJA2 phosphorylation, the canonical PKA substrate CREB was used as a control to confirm that the forskolin treatment worked. As expected, forskolin treatment showed a significant increase in phosphorylated CREB compared to DMSO control **(Figure 13B)**. However, forskolin treatment did not affect V5-PJA2 / FLAG-PJA2 interaction.

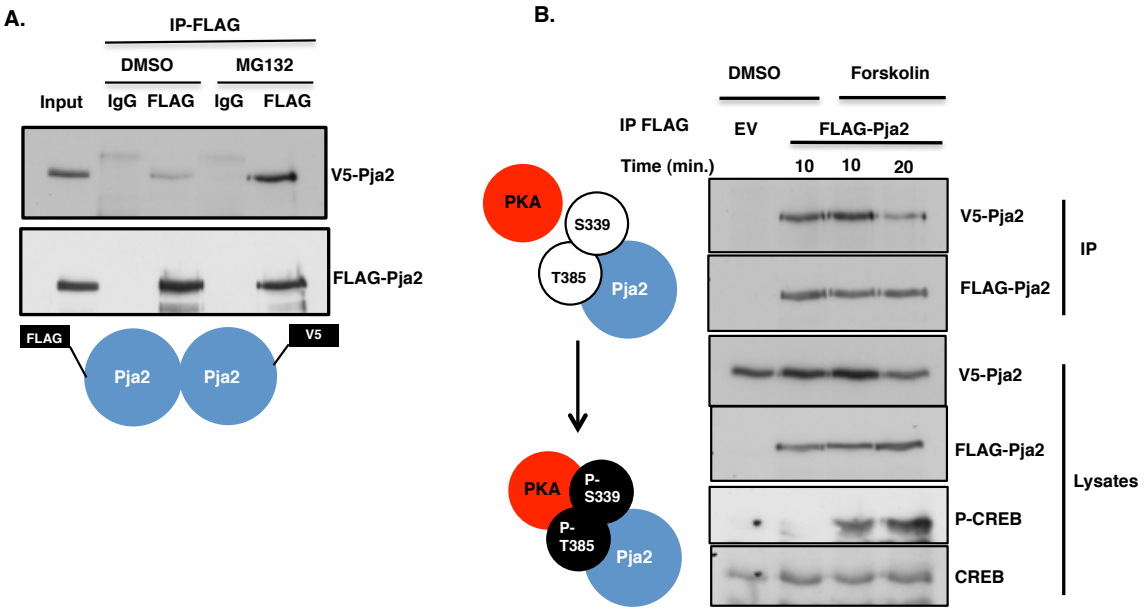
A.
IP-FLAG
DMSO
MG132
Input
IgG
FLAG
IgG
FLAG
V5-Pja2
FLAG-Pja2
FLAG
V5
Pja2
Pja2
B.
DMSO
Forskolin
IP FLAG
EV
FLAG-Pja2
Time (min.)
10
10
20
PKA
S339
T385
Pja2
V5-Pja2
FLAG-Pja2
IP
V5-Pja2
FLAG-Pja2
P-CREB
CREB
Lysates
PKA
P-S339
P-T385
Pja2

Figure 13. PJA2 undergoes self-interaction which is independent of cAMP signaling. **A.** Co-immunoprecipitation with flag-tagged PJA2 and V5-tagged PJA2 treated with their DMSO or MG132 for 8 hr prior to IP. **B.** Co-immunoprecipitation testing FLAG-tagged and V5-tagged PJA2 ability to self-interact after acute forskolin treatment. P-CREB was blotted to test for activation of PKA.

3.11 PJA2 interacts with p25 domain but not p10 domain of p35

In addition to self-interaction, Pja2's ability to interact with its substrate p35 was further characterized. Co-immunoprecipitation experiments of PJA2 and V5-p35 as well as reciprocal experiments of endogenous p35 and PJA2 demonstrated that the two proteins interact **(Appendix H)**. In addition, p35 can undergo calcium mediated calpain cleavage to generate two fragments termed p10 (n-terminal) and p25 (c-terminal). Interestingly, p25 was sufficient to bind and activate CDK5. Co-transfecting HEK 293T cells with PJA2 and either V5-p25 or V5-p10 reveals that PJA2 can interact with p25 fragment but not the n-terminal p10 fragment **(Figure 14A &14B)**. Interaction with V5-p35 was used as a positive control.

3.12 p35 interaction with PJA2 reduces auto-ubiquitination

Co-immunoprecipitation experiments from differentially tagged PJA2 suggest that PJA2 can undergo self-interaction. Furthermore, the data supports a model whereby PJA2 undergoes auto-ubiquitination, which provides a biological role for PJA2 self-interaction. In addition, PJA2 interaction with its substrate p35 occurs through the p25 domain. Given these PJA2 interaction profiles, the next logical step was to ask if PJA2 substrate interaction had an effect on its auto-ubiquitination capacity. Indeed, in vitro ubiquitination assays with GST-p35 showed reduced auto-ubiquitination capacity compared to GST alone **(Figure 15A)**. This effect was not dependent on p35 phosphorylation. Furthermore, a 4°C control confirmed that FLAG-PJA2 levels decreased as a result of the in vitro reaction.

Whether the p35 effect on PJA2 auto-ubiquitination was dependent on a specific domain of p35 still needed assessment. For this reason, GST-p10 and GST-p25 proteins were expressed and purified in bacteria and used in an in vitro ubiquitination reaction in the presence of FLAG-PJA2.

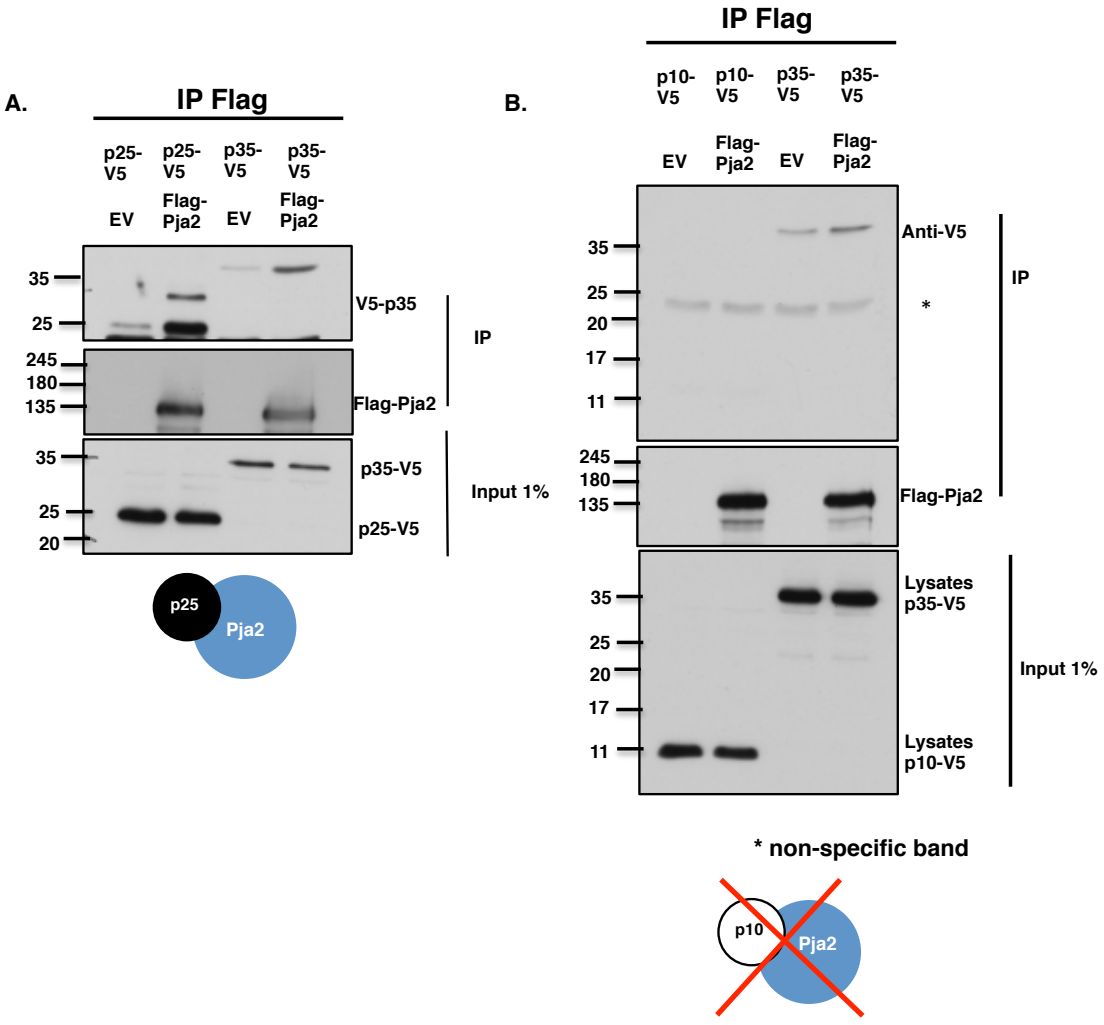
A.
IP Flag
p25-V5
p25-V5
p35-V5
p35-V5
EV
Flag-Pja2
EV
Flag-Pja2
35
25
245
180
135
35
25
20
V5-p35
Flag-Pja2
p35-V5
p25-V5
IP
Input 1%
p25
Pja2
B.
IP Flag
p10-V5
p10-V5
p35-V5
p35-V5
EV
Flag-Pja2
EV
Flag-Pja2
35
25
20
17
11
245
180
135
35
25
20
17
11
Anti-V5
*
Flag-Pja2
Lysates p35-V5
Lysates p10-V5
IP
Input 1%
* non-specific band
p10
Pja2

Figure 14. PJA2 interacts with p25 domain but not p10 domain of p35. FLAG-tagged PJA2 and p25-v5 **(A)** or p10-v5 **(B)** or p35-v5 positive control were transfected into HEK293T cells and FLAG-PJA2 was immunoprecipitated. After FLAG-PJA2 purification, lysates were separated on SDS-PAGE followed by blotting for FLAG-PJA2 and V5 constructs. A 1% input was run as control.

Surprisingly, GST alone, GST-p10 and GST-p25 all showed a comparable effect on PJA2 auto-ubiquitination. However, GST-p35 showed a significant reduction in PJA2 auto-ubiquitination as evidenced by the reduced smearing of higher molecular weight FLAG-PJA2 **(Figure 15B)**. Amido stain was used to assess levels of GST-tagged proteins. Collectively, these data support a model whereby PJA2 undergoes substrate-dependent *trans* auto-ubiquitination such that when p35-PJA2 interaction is high, PJA2 auto-ubiquitination is hampered **(Figure 15C)**.

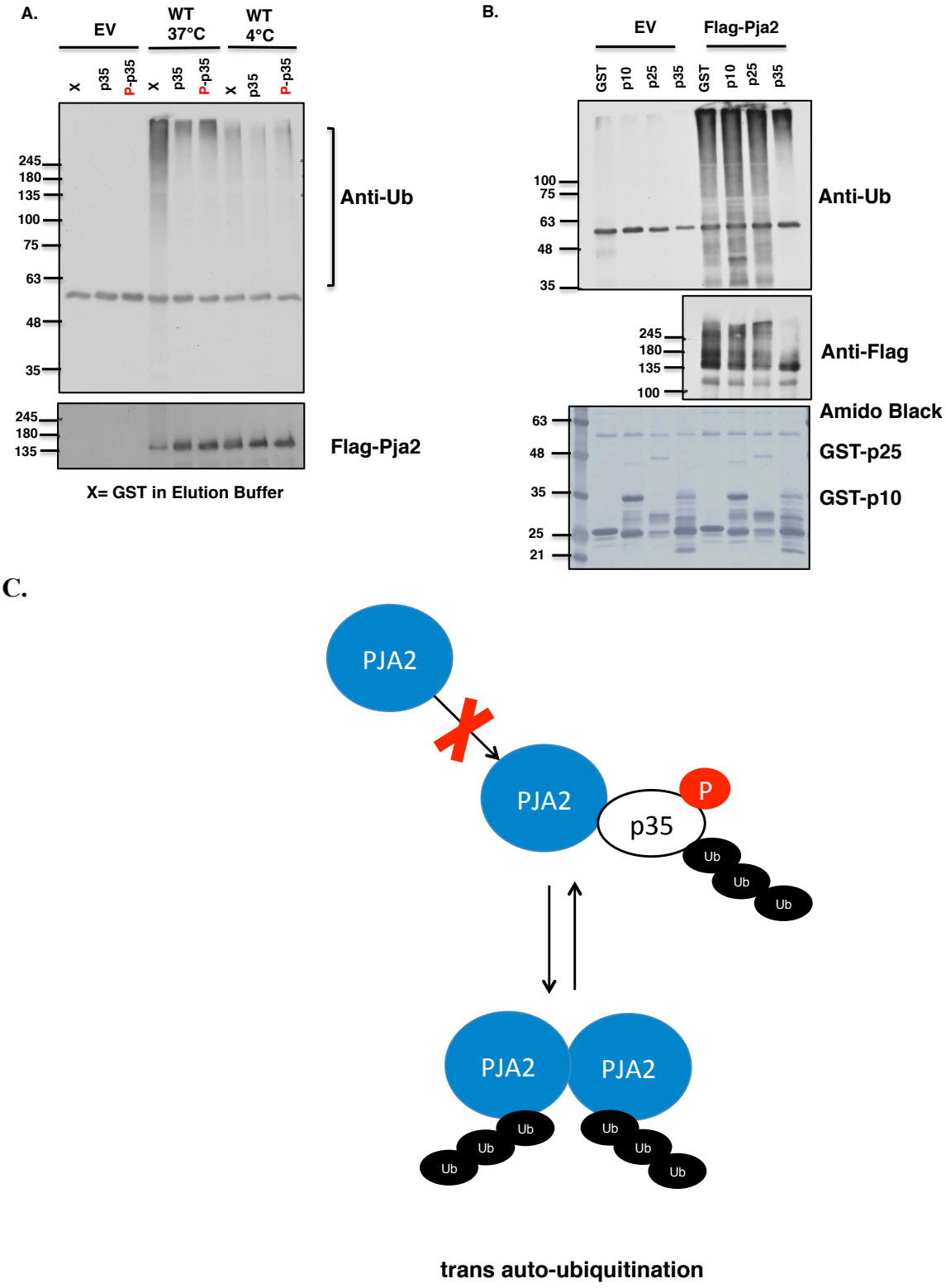
A.
EV
WT 37°C
WT 4°C
X
p35
P-p35
245
180
135
100
75
63
48
35
Anti-Ub
Flag-Pja2
X= GST in Elution Buffer
B.
EV
Flag-Pja2
GST
p10
p25
p35
Anti-Ub
Anti-Flag
Amido Black
GST-p25
GST-p10
C.
PJA2
P
p35
Ub
trans auto-ubiquitination

Figure 15. p35 interaction with PJA2 reduces auto-ubiquitination. (A) In vitro ubiquitination assay with empty vector or wild-type PJA2 in the presence of GST-p35, GST-p-p35, or GST control. Reaction was terminated with an equal volume 2X SDS after 60 min incubation at 37°C (or 4°C negative control). **(B)** In vitro ubiquitination assay with empty vector control or wild-type FLAG-PJA2 in the presence of GST control, or GST-p10, p25, or p35. Reaction was terminated with equal volume 2X SDS after 1 hr at 37°C .Samples were separated by SDS-PAGE before blotting for Ubiquitin and FLAG-PJA2. Amido black stain was used to assess levels of GST constructs. **(C)** Schematic illustration demonstrating the effect of p35 interaction on PJA2 auto-ubiquitination.

Chapter 4: Discussion

Sakamaki et al. elegantly established the role of SIK2-p35-PJA2 signaling cassette in pancreatic β-cell functional compensation in a recent Nature Cell Biology publication (65) . Thus emerged a novel signaling axis in β-cells that plays an important role in insulin secretion. Briefly, p35-CDK5 complex negatively regulates voltage-dependent calcium channel activity resulting in reduced calcium influx with a concomitant reduction in insulin secretion (65, 70). The AMPK family member kinase SIK2 phosphorylates p35 at Ser91 resulting in ubiquitination by the E3 ligase PJA2 and subsequent degradation via the proteasome system. Interestingly, SIK2 levels are stabilized by long-term glucose treatment, which further supports its role in β-cell functional compensation. p35 is arguably the most important component of this signaling cascade, behaving as a central node that interconnects CDK5, SIK2, and PJA2. By this logic, identifying novel genes that regulate p35 levels could further elucidate the pathway. This rationale essentially prompted the use of immunoprecipitation-coupled mass spectrometry to identify p35 interactor genes. The approach garnered confidence after successfully identifying the canonical p35 interacting protein CDK5 as a candidate interacting protein. Afterwards, high-throughput RNAi based screen was used in order to test for legitimate candidate genes that regulate p35 levels. Although a powerful technique, high-throughput RNAi based screening comes with its drawbacks. For example, use of RNAi introduces the possibility of off-target effects, which need to be minimized to observe the true phenotype of genetic knockdown. Our approach of overcoming this caveat was to generate multiple shRNA per gene of interest and only proceed with a candidate when at least 2 shRNA were in agreement. A second drawback of the screen was cytotoxic effects that can mask the true phenotype. If the gene of interest is

important for cell health, loss of the gene will result in impaired cell viability. In addition, improper virus preparation can result in cytotoxic effects that can introduce an extra layer of confounding variables as to the source of toxicity. Most importantly, high-throughput screens by their nature are characterized with an element of speed and often only allow a single output. When designing a screen, it's important to select an appropriate readout and an ideal means to obtain it. For example, the readout that was used for the above mentioned screen was endogenous p35 levels as assayed by western. Other potential outputs that could have been used for the screen include p35 phosphorylation state as assayed by phosho-p35 specific antibody, p35 localization as assayed by IF, or even p35 ubiquitination. However, it is important to take into consideration the resources at one's disposal.

The most promising candidate from the high-throughput RNAi screen was a chaperone protein called RNA polymerase II associated protein 3 (RPAP3). Indeed RPAP3 knockdown with two independent shRNA resulted in p35 elevation (**Figure 2A)**. However, the expected effect of decreased insulin secretion associated with elevated p35 was never reliably observed. This prompts the question: why does p35 elevation reduce insulin secretion in one context but not others? There are several interpretations but one possibility is that there is an uncoupling between p35 levels and insulin secretion in MIN6 cells. Another interpretation follows the logic that RPAP3 has multiple functions in the cell and loss of RPAP3 results in multiple phenotypes only one of which is p35 elevation. Therefore, loss of RPAP3 could be associated with other unknown phenotypes which overcome the expected insulin secretion defect. Certainly RPAP3's role as a co-chaperone in several key pathways further supports the multiple functions assumption (56, 57). The same thinking can be applied to the E3 ligase PJA2.

It is established that knockdown of PJA2 results in elevated p35 levels. Furthermore, PJA2 overexpression is associated with reduced endogenous p35. In addition, in vitro ubiquitination assays have demonstrated that PJA2 was able to ubiquitinate the substrate GST-p35. Collectively, these data implicate PJA2 as a bona fide E3 ligase of p35. At the same time, PJA2 has been reported to ubiquitinate multiple substrates including PKA regulatory subunits, MOB1, and NOGO-A (35, 107, 108). Not much is known about PJA2 but what little is available suggests that it plays important roles in calcium, cAMP, and Hippo signaling.

It is important to understand the rationale behind the research presented herein; namely, p35 levels in β-cells can regulate insulin secretion such that elevated p35 levels results in reduced insulin secretion and vice versa. Secondly, genes that regulate p35 levels will also regulate insulin secretion. In a diabetes context, the ultimate objective is to restore normoglycemia and as is often the case, this requires improving β-cell function. Therefore, it becomes worthwhile to explore mechanisms of increasing insulin secretion in order to meet the demands of a hyperglycemic environment. Considering that the most blaring evidence of p35 regulation thus far implicates PJA2, one would logically hypothesize that modulating PJA2 levels could help regulate insulin secretion. Indeed knockdown of PJA2 results in a dramatic decrease in insulin secretion **(Figure 3B)**. The more intriguing question asks if PJA2 overexpression could enhance insulin secretion. The best interpretation of the data thus far suggests that PJA2 overexpression does not significantly affect insulin secretion. Immunofluorescence of MIN6 cells infected with lentivirus overexpressing either PJA2 constructs or an empty vector control demonstrates a high infection rate (**Figure 8)**. One can argue that the degree of infection is heterogeneous in the wild-type condition and that the population of uninfected cells could be masking the insulin secretion phenotype. To address

this specific concern, PJA2 constructs were cloned into an 'attenuated expression vector' termed Δ4 CMV in order reduce promoter function and increase homogeneous expression. As verified by western, the attenuated vector was able to overexpress 2CA and K3R PJA2 mutants to near endogenous levels **(Figure 12B)**. However, no change in insulin secretion was observed despite a significant reduction in p35 levels by the K3R mutant. One possibility is that MIN6 cells are highly sensitive to the 20 mM glucose stimulus and thus secrete insulin at a maximum rate such that PJA2 modulation of insulin secretion becomes indiscernible. To overcome this, MIN6 cells were subjected to lower concentrations of glucose as stimulus for insulin secretion. Interestingly, 2CA and K3R mutants showed significant increase in insulin secretion at 20 mM glucose stimulus whereas all PJA2 constructs showed an increased trend in insulin secretion in both the 11 mM and 20 mM glucose stimulus. It is unclear why this increase in insulin secretion was significant. One confounding variable inherent in this format of the GSIS experiment compared to the traditional GSIS is the longer starvation period. Whereas in the traditional GSIS, cells are starved in 1mM glucose before stimulation with 20mM glucose, the glucose titer format involves incubation with 1mM glucose followed by an incubation with 5.5 mM glucose before the final two incubations with 11 mM and 20 mM glucose. It is possible that the presence of PJA2 confers some advantage to β-cell function which becomes apparent after longer periods of starvation. Interestingly, doubling virus concentration of PJA2 constructs and increasing incubation time results in significantly reduced insulin secretion independent of E3 ligase activity **(Figure 11A&B)**. PJA2 is a reported A-kinase anchoring protein (AKAP) that functions by targeting PKA to 'specific intracellular microdomains' (107, 114). In this manner, PJA2-PKA interaction plays an important role in locally controlling cAMP signaling through PKA. Therefore, the observation that overt PJA2 overexpression causes

reduced insulin secretion independent of enzymatic activity can be explained by the AKAP functionality of PJA2. It is possible that endogenous PJA2, as defined by its role as an AKAP, must undergo tight regulation in highly localized microdomains. In theory, overexpression of PJA2 can disrupt its intracellular localization and consequently deregulate cAMP-PKA signal transduction. The link between PKA activation and enhanced insulin secretion is robust (39, 60) [reviewed in (89)]. In fact, PKA activation through the GLP-1 agonist Exendin-4 is used to improve insulin secretion in Type II diabetics. Of course, there are PKA-independent effects of GLP-1 on insulin secretion such as guanine nucleotide exchange factors (GEFs) [reviewed in (98)]. Nevertheless, PKA deregulation arising from PJA2 overexpression could clarify the unexpected phenotype of reduced insulin secretion and explain why the cell tightly regulates PJA2 levels.

In addition to implicating PJA2 as an AKAP, Lignitto and colleagues propose that PJA2 activity is reciprocally activated by PKA through phosphorylation of Ser339 and Thr385. They further add that this feed-forward signaling cascade plays an important role in PKA-mediated long-term memory formation. Our data supports an additional mode of PJA2 regulation. Namely, PJA2 undergoes auto-ubiquitination as evidenced by MG132 mediated stabilization of PJA2, stabilization of catalytically inactive PJA2, as well as in vitro auto-ubiquitination assays **(Figure 6, Appendix C)**.

Prefaced with the idea that PJA2 overexpression could therapeutically enhance β-cell function, we sought to identify potential auto-ubiquitination sites. The benefits of using a bioinformatics approach to identify post-translational modifications such as ubiquitination are manifold not the least of which are its simplicity and time/cost-effectiveness. However, the post-translational modification databases used to identify lysines K317, K336, and K666 as potential auto-ubiquitination sites were unfruitful. More specifically, mutating these 3

residues individually or in permutations thereof did not significantly stabilize PJA2 relative to the positive control 2CA mutant **(Figure 5)**. One possible explanation is that these reported sites are legitimate ubiquitination sites that may not be important for PJA2 degradation. Indeed there are several forms of polyubiquitination of which only lysine-48 linkage is associated with proteasomal degradation. Ideally, mass spectrometry can be used to identify sites of ubiquitination however this resource is often not readily available. In addition, not all identified ubiquitination sites may be important for degradation and thus must be tested empirically. There are multiple resources that predict ubiquitination sites based on patterns observed from previously reported sites however they are often unreliable. It is also unreasonable to rely on a strict trial-and-error approach especially in the context of lysine-rich proteins such as PJA2.

Co-immunoprecipitation experiments reveal that PJA2 can self-interact **(Figure 13A)** supporting the model that PJA2 undergoes *trans* mediated auto-ubiquitination. It is important to differentiate between *cis* and *trans* mediated auto-ubiquitination if one wants to explore lysines in the RING domain as potential auto-ubiquitination sites. The RING domain functions by coordinating the ubiquitination of lysine residues. Therefore it is unlikely that an E3 ligase that undergoes cis auto-ubiquitination will be able to ubiquitinate lysine residues in the RING domain due to the fact that the RING domain itself is necessary for the process of ubiquitination. Of course this may not be true if a single E3 ligase possesses multiple RING domains. In the case of *trans* auto-ubiquitination, the presence of two E3 ligases and thus two RING domains allows one to potentially coordinate the ubiquitination of lysines in the other. Interestingly, PJA2 RING domain is highly conserved between species **(Appendix E)**. Furthermore, there is 100% conservation in the RING domain between mPJA2 and its homologue mPJA1. In addition, K666 in the RING domain of PJA2 was among the reported

lysines to undergo ubiquitination further supporting the hypothesis that PJA2 auto-ubiquitination sites can be found in the RING domain.

In fact, a triple mutant of lysines (K3R) situated in the RING domain of PJA2 demonstrates significant stabilization compared to wild-type PJA2 **(Figure 6)**. Moreover, this stabilization of the K3R mutant is associated with a reduced capacity to undergo auto-ubiquitination. Although the K3R mutant demonstrates comparable stabilization to the 2CA mutant, it still demonstrates some degree of auto-ubiquitination. One likely interpretation of this observation is that PJA2-K3R mutant still has other lysines that can undergo ubiquitination. Nevertheless, the observation that K3R/2CA stability is comparable suggests that the other unidentified lysines may not be important for PJA2 degradation. An obvious concern is that mutating residues in a catalytic domain will compromise the enzymatic activity of PJA2. More specifically, mutating residues in the RING domain of an E3 ligase can theoretically affect the ability of the enzyme to ubiquitinate substrates. In the case of PJA2, cysteine to alanine mutations of C633 and C670 results in RING destabilization resulting in abolished enzymatic activity. However, the similarities between lysine (K) and arginine (R) residues allow K to R mutations to maintain the 3D structural integrity of the mutated protein. In fact, 8 lysine to arginine mutations in the RING domain of Trim17 did not significantly affect E3 ligase activity (55). Similarly, mutating the RING domain lysine in BCA2 maintained normal E3 ligase activity (58). In agreement, our data demonstrates that 3 lysine to arginine mutations in the RING domain of PJA2 did not significantly affect enzymatic activity compared to wild-type PJA2 **(Figure 7a-c)**. However, the data equally supports the model that PJA2-K3R demonstrates a slight deficit in enzymatic activity. In addition, the ubiquitination assays show an unequal amount of WT and K3R PJA2, which in actuality supports the outcome that on a per molecule basis, wild-type PJA2 has enhanced

activity compared to K3R mutant. This effect is not apparent in vivo where K3R-PJA2 demonstrates greater regulation of endogenous p35 compared to the wild-type **(Appendix G).**

Thus far, the p35-PJA2 dynamic has been examined in a linear manner. More specifically, the proposed model emphasizes that PJA2 regulates p35 levels through ubiquitin-mediated degradation. An intriguing set of data sheds light on the potential reciprocal nature of p35-PJA2 interactions. In fact, in vitro ubiquitination assay demonstrates that PJA2 undergoes reduced auto-ubiquitination in the presence of GST-p35 but not GST-control (**Figure 15A)**. Interestingly, the reduced auto-ubiquitination capacity is only observed with GST-p35 but not in the presence of GST-p10 or GST-p25. However, co-immunoprecipitation experiments further characterized the p35-PJA2 dynamic by implicating p25 to be sufficient for PJA2 interaction **(Figure 14)**. Given this, one could argue that the PJA2 binding fragment of p25 should be sufficient to promote reduced auto-ubiquitination of PJA2. One possibility is that the p35 effect on PJA2 auto-ubiquitination requires the full-length protein. There could be an important fragment situated between p10 and p25 that is necessary for attenuating PJA2 auto-ubiquitination. In addition, these interpretations could be confounded by the large 26 kDa GST-tag that could interfere with PJA2-p35 interaction. Nevertheless, the idea that p35 attenuates PJA2 auto-ubiquitination is logically sound when structured under the context that the primary function of E3 ligases is to ubiquitinate substrates. On the contrary, one could argue this effect to be an artifact of in vitro ubiquitination that may not have any biological significance. In a cell biological context where proteins are tightly regulated, p35 levels may never rise beyond the threshold required to impact PJA2 auto-ubiquitination. Interestingly, Bacopulos et al. demonstrated that interaction between the E3 ligase BCA2 and its substrate 14-3-3σ promoted BCA2

stabilization (59). Furthermore, they show that BCA2- 14-3-3σ interaction is dependent on AKT phosphorylation of BCA2. In doing so, they provide evidence that E3 ligase-substrate interaction can promote E3 ligase stabilization in an in vivo context. In addition, Ranaweera and Yang demonstrated that Mdm2 auto-ubiquitination promoted enhanced substrate ubiquitination of p53 (111). They reasoned that Mdm2 auto-ubiquitination generated polyubiquitin chains, which recruited E2 conjugating enzyme. Afterwards, the increased localization of E2-E3-substrate promoted enhanced processing of substrate ubiquitination. Interestingly, this suggests that PJA2 auto-ubiquitination may enhance p35 ubiquitination. More importantly, lack of auto-ubiquitination as seen in the K3R mutant could explain its reduced capacity to ubiquitinate p35.

Conclusion

In summary, this thesis explores the E3 ligase-substrate dynamics of PJA2-p35 in the context of β-cell function. Loss of PJA2 causes elevated p35 levels, reduced Ca^{2+} influx and concomitant decrease in insulin secretion. I sought to test the alternative side of the model, namely that PJA2 overexpression will promote enhanced β-cell function. I was able to confirm the auto-ubiquitination properties of PJA2 and generate a stable PJA2 mutant that undergoes reduced auto-ubiquitination. Furthermore, I demonstrated the activity of the K3R mutant to be intact as compared to wild-type PJA2 and 2CA mutant. However, the effect of PJA2 overexpression in insulin secretion was determined to be non-significant. In the absence of an effect on insulin secretion following PJA2 overexpression, it may not be worthwhile to pursue a β-cell specific PJA2 transgenic mouse. Future screening efforts will benefit from using the biological function of insulin secretion as readout to identify genes which have direct impact in β-cell function.

References

1. **Rosenfeld L.** 2002. Insulin: discovery and controversy. Clinical Chemistry **48:**2270-2288.
2. **Watson RT, Kanzaki M, Pessin JE.** 2004. Regulated membrane trafficking of the insulin-responsive glucose transporter 4 in adipocytes. Endocrine Reviews **25:**177-204.
3. **Shapiro AMJ, Lakey JRT, Ryan EA, Korbutt GS, Toth E, Warnock GL, Kneteman NM, Rajotte RV.** 2000. Islet transplantation in seven patients with type 1 diabetes mellitus using a glucocorticoid-free immunosuppressive regimen. New England Journal of Medicine **343:**230-238.
4. **Ryan EA, Paty BW, Senior PA, Bigam D, Alfadhli E, Kneteman NM, Lakey JRT, Shapiro AMJ.** 2005. Five-year follow-up after clinical islet transplantation. Diabetes **54:**2060-2069.
5. **Shapiro AMJ, Ricordi C, Hering BJ, Auchincloss H, Lindblad R, Robertson RP, Secchi A, Brendel MD, Berney T, Brennan DC, Cagliero E, Alejandro R, Ryan EA, DiMercurio B, Morel P, Polonsky KS, Reems JA, Bretzel RG, Bertuzzi F, Froud T, Kandaswamy R, Sutherland DER, Eisenbarth G, Segal M, Preiksaitis J, Korbutt GS, Barton FB, Viviano L, Seyfert-Margolis V, Bluestone J, Lakey JRT.** 2006. International trial of the Edmonton protocol for islet transplantation. New England Journal of Medicine **355:**1318-1330.
6. **Gepts W.** 1965. Pathologic anatomy of the pancreas in juvenile diabetes mellitus. Diabetes **14:**619-633.
7. **Mathis D, Vence L, Benoist C.** 2001. β-cell death during progression to diabetes. Nature **414:**792-798.
8. **Van Belle TL, Coppieters KT, Von Herrath MG.** 2011. Type 1 diabetes: Etiology, immunology, and therapeutic strategies. Physiological Reviews **91:**79-118.
9. **Bluestone JA, Herold K, Eisenbarth G.** 2010. Genetics, pathogenesis and clinical interventions in type 1 diabetes. Nature **464:**1293-1300.
10. **Barker JM.** 2006. Type 1 diabetes-associated autoimmunity: Natural history, genetic associations, and screening. Journal of Clinical Endocrinology and Metabolism **91:**1210-1217.
11. **Anderson MS, Bluestone JA.** 2005. The NOD mouse: A model of immune dysregulation, p. 447-485, Annual Review of Immunology, vol. 23.
12. **Roep BO.** 2003. The role of T-cells in the pathogenesis of Type 1 diabetes: From cause to cure. Diabetologia **46:**305-321.
13. **Imagawa A, Hanafusa T, Miyagawa JI, Matsuzawa Y.** 2000. A proposal of three distinct subtypes of type 1 diabetes mellitus based on clinical and pathological evidence. Annals of Medicine **32:**539-543.
14. **Shaw JE, Sicree RA, Zimmet PZ.** 2010. Global estimates of the prevalence of diabetes for 2010 and 2030. Diabetes Research and Clinical Practice **87:**4-14.
15. **Tuomilehto J, Lindstr√ ∂ m J, Eriksson JG, Valle TT, Ham√ § l√ § inen H, Ianne-Parikka P, Kein√ § nen-Kiukaanniemi S, Laakso M, Louheranta A, Rastas M, Salminen V, Uusitupa M.** 2001. Prevention of type 2 diabetes

mellitus by changes in lifestyle among subjects with impaired glucose tolerance. New England Journal of Medicine **344:**1343-1350.
16. **McCarthy MI.** 2010. Genomics, type 2 diabetes, and obesity. New England Journal of Medicine **363:**2339-2350.
17. **Hamilton MT, Hamilton DG, Zderic TW.** 2007. Role of low energy expenditure and sitting in obesity, metabolic syndrome, type 2 diabetes, and cardiovascular disease. Diabetes **56:**2655-2667.
18. **Yoon KH, Lee JH, Kim JW, Cho JH, Choi YH, Ko SH, Zimmet P, Son HY.** 2006. Epidemic obesity and type 2 diabetes in Asia. Lancet **368:**1681-1688.
19. **Kahn SE, Hull RL, Utzschneider KM.** 2006. Mechanisms linking obesity to insulin resistance and type 2 diabetes. Nature **444:**840-846.
20. **Hannon TS, Rao G, Arslanian SA.** 2005. Childhood obesity and type 2 diabetes mellitus. Pediatrics **116:**473-480.
21. **Lingohr MK, Buettner R, Rhodes CJ.** 2002. Pancreatic β-cell growth and survival - A role in obesity-linked type 2 diabetes? Trends in Molecular Medicine **8:**375-384.
22. **Greenberg AS, McDaniel ML.** 2002. Identifying the links between obesity, insulin resistance and β-cell function: Potential role of adipocyte-derived cytokines in the pathogenesis of type 2 diabetes. European Journal of Clinical Investigation **32:**24-34.
23. **Maggio CA, Pi-Sunyer FX.** 1997. The prevention and treatment of obesity: Application to type 2 diabetes. Diabetes Care **20:**1744-1766.
24. **Andersen S, Fleischer Rex K, Noahsen P, Florian Sørensen HC, Mulvad G, Laurberg P.** 2013. Raised BMI cut-off for overweight in Greenland Inuit - A review. International Journal of Circumpolar Health **72**.
25. **Werner D, Teufel J, Holtgrave PL, Brown SL.** 2012. Active generations: An intergenerational approach to preventing childhood obesity. Journal of School Health **82:**380-386.
26. **Nguyen T, Lau DCW.** 2012. The Obesity Epidemic and Its Impact on Hypertension. Canadian Journal of Cardiology **28:**326-333.
27. **Lang JE.** 2012. Obesity, nutrition, and asthma in children. Pediatric, Allergy, Immunology, and Pulmonology **25:**64-75.
28. **Karasu SR.** 2012. Of mind and matter: Psychological dimensions in obesity. American Journal of Psychotherapy **66:**111-128.
29. **Singh-Manoux A, Gourmelen J, Lajnef M, Sabia S, Sitta R, Menvielle G, Melchior M, Nabi H, Lanoe JL, Guéguen A, Lert F.** 2009. Prevalence of educational inequalities in obesity between 1970 and 2003 in France. Obesity Reviews **10:**511-518.
30. **Westerterp KR, Speakman JR.** 2008. Physical activity energy expenditure has not declined since the 1980s and matches energy expenditures of wild mammals. International Journal of Obesity **32:**1256-1263.
31. **Wardle J, Boniface D.** 2008. Changes in the distributions of body mass index and waist circumference in English adults, 1993/1994 to 2002/2003. International Journal of Obesity **32:**527-532.

32. **Steppan CM, Bailey ST, Bhat S, Brown EJ, Banerjee RR, Wright CM, Patel HR, Ahima RS, Lazar MA.** 2001. The hormone resistin links obesity to diabetes. Nature **409:**307-312.
33. **Wellen KE, Hotamisligil GS.** 2005. Inflammation, stress, and diabetes. Journal of Clinical Investigation **115:**1111-1119.
34. **Cefalu WT.** 2001. Insulin resistance: Cellular and clinical concepts. Proceedings of the Society for Experimental Biology and Medicine **226:**13-26.
35. **Wen H, Gris D, Lei Y, Jha S, Zhang L, Huang MTH, Brickey WJ, Ting JPY.** 2011. Fatty acid-induced NLRP3-ASC inflammasome activation interferes with insulin signaling. Nature Immunology **12:**408-415.
36. **Özcan U, Cao Q, Yilmaz E, Lee AH, Iwakoshi NN, Özdelen E, Tuncman G, Görgün C, Glimcher LH, Hotamisligil GS.** 2004. Endoplasmic reticulum stress links obesity, insulin action, and type 2 diabetes. Science **306:**457-461.
37. **Nakatani Y, Kaneto H, Kawamori D, Yoshiuchi K, Hatazaki M, Matsuoka TA, Ozawa K, Ogawa S, Hori M, Yamasaki Y, Matsuhisa M.** 2005. Involvement of endoplasmic reticulum stress in insulin resistance and diabetes. Journal of Biological Chemistry **280:**847-851.
38. **Moran A, Jacobs Jr DR, Steinberger J, Hong CP, Prineas R, Luepker R, Sinaiko AR.** 1999. Insulin resistance during puberty: Results from clamp studies in 357 children. Diabetes **48:**2039-2044.
39. **Weiss R, Bremer AA, Lustig RH.** 2013. What is metabolic syndrome, and why are children getting it?, p. 123-140, Annals of the New York Academy of Sciences, vol. 1281.
40. **Eberhard D.** 2013. Neuron and beta-cell evolution: Learning about neurons is learning about beta-cells. BioEssays **35:**584.
41. **Martens GA, Jiang L, Hellemans KH, Stangé G, Heimberg H, Nielsen FC, Sand O, van Helden J, Gorus FK, Pipeleers DG.** 2011. Clusters of conserved beta cell marker genes for assessment of beta cell phenotype. PLoS ONE **6**.
42. **Van Arensbergen J, García-Hurtado J, Moran I, Maestro MA, Xu X, Van De Casteele M, Skoudy AL, Palassini M, Heimberg H, Ferrer J.** 2010. Derepression of polycomb targets during pancreatic organogenesis allows insulin-producing beta-cells to adopt a neural gene activity program. Genome Research **20:**722-732.
43. **Dioum EM, Osborne JK, Goetsch S, Russell J, Schneider JW, Cobb MH.** 2011. A small molecule differentiation inducer increases insulin production by pancreatic β cells. Proceedings of the National Academy of Sciences of the United States of America **108:**20713-20718.
44. **Oomura Y, Kimura K, Ooyama H, Maeno T, Matasaburo I, Kuniyoshi M.** 1964. Reciprocal activities of the ventromedial and lateral hypothalamic areas of cats. Science **143:**484-485.
45. **Anand BK, Chhina GS, Sharma KN, Dua S, Singh B.** 1964. ACTIVITY OF SINGLE NEURONS IN THE HYPOTHALAMIC FEEDING CENTERS: EFFECT. The American journal of physiology **207:**1146-1154.
46. **Levin BE, Routh VH, Kang L, Sanders NM, Dunn-Meynell AA.** 2004. Neuronal glucosensing: What do we know after 50 years? Diabetes **53:**2521-2528.

47. **Parton LE, Ye CP, Coppari R, Enriori PJ, Choi B, Zhang CY, Xu C, Vianna CR, Balthasar N, Lee CE, Elmquist JK, Cowley MA, Lowell BB.** 2007. Glucose sensing by POMC neurons regulates glucose homeostasis and is impaired in obesity. Nature **449:**228-232.
48. **Efrat S.** 1997. Making sense of glucose sensing. Nature Genetics **17:**249-250.
49. **Kellett GL, Brot-Laroche E, Mace OJ, Leturque A.** 2008. Sugar absorption in the intestine: The role of GLUT2, p. 35-54, Annual Review of Nutrition, vol. 28.
50. **Kellett GL, Brot-Laroche E.** 2005. Apical GLUT2: A major pathway of intestinal sugar absorption. Diabetes **54:**3056-3062.
51. **Freitas HS, D'Agord Schaan B, Seraphim PM, Nunes MT, Machado UF.** 2005. Acute and short-term insulin-induced molecular adaptations of GLUT2 gene expression in the renal cortex of diabetic rats. Molecular and Cellular Endocrinology **237:**49-57.
52. **Matschinsky FM.** 1990. Glucokinase as glucose sensor and metabolic signal generator in pancreatic β-cells and hepatocytes. Diabetes **39:**647-652.
53. **German MS.** 1993. Glucose sensing in pancreatic islet beta cells: The key role of glucokinase and the glycolytic intermediates. Proceedings of the National Academy of Sciences of the United States of America **90:**1781-1785.
54. **Zheng YL, Hu YF, Zhang A, Wang W, Li B, Amin N, Grant P, Pant HC.** 2010. Overexpression of p35 in Min6 pancreatic beta cells induces a stressed neuron-like apoptosis. Journal of the Neurological Sciences **299:**101-107.
55. **Fu A, Eberhard CE, Screaton RA.** 2013. Role of AMPK in pancreatic beta cell function. Molecular and Cellular Endocrinology **366:**127-134.
56. **Pagliuca FW, Millman JR, Gürtler M, Segel M, Van Dervort A, Ryu JH, Peterson QP, Greiner D, Melton DA.** 2014. Generation of functional human pancreatic β cells in vitro. Cell **159:**428-439.
57. **Fryer BH, Rezania A, Zimmerman MC.** 2013. Generating β-cells in vitro: Progress towards a Holy Grail. Current Opinion in Endocrinology, Diabetes and Obesity **20:**112-117.
58. **Nostro MC, Keller G.** 2012. Generation of beta cells from human pluripotent stem cells: Potential for regenerative medicine. Seminars in Cell and Developmental Biology **23:**701-710.
59. **Criscimanna A, Zito G, Taddeo A, Richiusa P, Pitrone M, Morreale D, Lodato G, Pizzolanti G, Citarrella R, Galluzzo A, Giordano C.** 2012. In vitro generation of pancreatic endocrine cells from human adult fibroblast-like limbal stem cells. Cell Transplantation **21:**73-90.
60. **Champeris Tsaniras S, Jones PM.** 2010. Generating pancreatic β-cells from embryonic stem cells by manipulating signaling pathways. Journal of Endocrinology **206:**13-26.
61. **Smukler SR, Arntfield ME, Razavi R, Bikopoulos G, Karpowicz P, Seaberg R, Dai F, Lee S, Ahrens R, Fraser PE, Wheeler MB, Van Der Kooy D.** 2011. The adult mouse and human pancreas contain rare multipotent stem cells that express insulin. Cell Stem Cell **8:**281-293.
62. **Sachdeva MM, Stoffers DA.** 2009. Minireview: Meeting the demand for insulin: Molecular mechanisms of adaptive postnatal Œ≤-cell mass expansion. Molecular Endocrinology **23:**747-758.

63. **Asghar Z, Yau D, Chan F, LeRoith D, Chan CB, Wheeler MB.** 2006. Insulin resistance causes increased beta-cell mass but defective glucose-stimulated insulin secretion in a murine model of type 2 diabetes. Diabetologia **49:**90-99.
64. **Gonzalez A, Merino B, Marroqu√ ≠ L, √ ëeco P, Alonso-Magdalena P, Caballero-Garrido E, Vieira E, Soriano S, Gomis R, Nadal A, Quesada I.** 2013. Insulin hypersecretion in islets from diet-induced hyperinsulinemic obese female mice is associated with several functional adaptations in individual Œ≤-cells. Endocrinology **154:**3515-3524.
65. **Sakamaki JI, Fu A, Reeks C, Baird S, Depatie C, Azzabi MA, Bardeesy N, Gingras AC, Yee SP, Screaton RA.** 2014. Role of the SIK2-p35-PJA2 complex in pancreatic β-cell functional compensation (Nature Cell Biological (2014) 16, 234-244). Nature Cell Biology **16:**382.
66. **Chang AM, Halter JB.** 2003. Aging and insulin secretion. American Journal of Physiology - Endocrinology and Metabolism **284:**E7-E12.
67. **Belgardt BF, Stoffel M.** 2014. SIK2 regulates insulin secretion. Nature Cell Biology **16:**210-212.
68. **Lilja L, Johansson JU, Gromada J, Mandic SA, Fried G, Berggren PO, Bark C.** 2004. Cyclin-dependent kinase 5 associated with p39 promotes Munc18-1 phosphorylation and Ca2+-dependent exocytosis. Journal of Biological Chemistry **279:**29534-29541.
69. **Lilja L, Yang SN, Webb DL, Juntti-Berggren L, Berggren PO, Bark C.** 2001. Cyclin-dependent Kinase 5 Promotes Insulin Exocytosis. Journal of Biological Chemistry **276:**34199-34205.
70. **Wei FY, Nagashima K, Ohshima T, Saheki Y, Lu YF, Matsushita M, Yamada Y, Mikoshiba K, Seino Y, Matsui H, Tomizawa K.** 2005. Cdk5-dependent regulation of glucose-stimulated insulin secretion. Nature Medicine **11:**1104-1108.
71. **Zhou G, Myers R, Li Y, Chen Y, Shen X, Fenyk-Melody J, Wu M, Ventre J, Doebber T, Fujii N, Musi N, Hirshman MF, Goodyear LJ, Moller DE.** 2001. Role of AMP-activated protein kinase in mechanism of metformin action. Journal of Clinical Investigation **108:**1167-1174.
72. **Winder WW, Hardie DG.** 1999. AMP-activated protein kinase, a metabolic master switch: Possible roles in Type 2 diabetes. American Journal of Physiology - Endocrinology and Metabolism **277:**E1-E10.
73. **Hawley SA, Pan DA, Mustard KJ, Ross L, Bain J, Edelman AM, Frenguelli BG, Hardie DG.** 2005. Calmodulin-dependent protein kinase kinase-β is an alternative upstream kinase for AMP-activated protein kinase. Cell Metabolism **2:**9-19.
74. **Stein SC, Woods A, Jones NA, Davison MD, Cabling D.** 2000. The regulation of AMP-activated protein kinase by phosphorylation. Biochemical Journal **345:**437-443.
75. **Woods A, Johnstone SR, Dickerson K, Leiper FC, Fryer LGD, Neumann D, Schlattner U, Wallimann T, Carlson M, Carling D.** 2003. LKB1 Is the Upstream Kinase in the AMP-Activated Protein Kinase Cascade. Current Biology **13:**2004-2008.

76. **Oakhill JS, Steel R, Chen ZP, Scott JW, Ling N, Tam S, Kemp BE.** 2011. AMPK is a direct adenylate charge-regulated protein kinase. Science **332:**1433-1435.
77. **Xiao B, Sanders MJ, Underwood E, Heath R, Mayer FV, Carmena D, Jing C, Walker PA, Eccleston JF, Haire LF, Saiu P, Howell SA, Aasland R, Martin SR, Carling D, Gamblin SJ.** 2011. Structure of mammalian AMPK and its regulation by ADP. Nature **472:**230-233.
78. **Screaton RA, Conkright MD, Katoh Y, Best JL, Canettieri G, Jeffries S, Guzman E, Niessen S, Yates Iii JR, Takemori H, Okamoto M, Montminy M.** 2004. The CREB coactivator TORC2 functions as a calcium- and cAMP-sensitive coincidence detector. Cell **119:**61-74.
79. **Dentin R, Liu Y, Koo SH, Hedrick S, Vargas T, Heredia J, Yates Iii J, Montminy M.** 2007. Insulin modulates gluconeogenesis by inhibition of the coactivator TORC2. Nature **449:**366-369.
80. **Horike N, Takemori H, Katoh Y, Doi J, Min L, Asano T, Sun XJ, Yamamoto H, Kasayama S, Muraoka M, Nonaka Y, Okamoto M.** 2003. Adipose-specific expression, phosphorylation of Ser794 in insulin receptor substrate-1, and activation in diabetic animals of salt-inducible kinase-2. Journal of Biological Chemistry **278:**18440-18447.
81. **Sun XJ, Goldberg JL, Qiao LY, Mitchell JJ.** 1999. Insulin-induced insulin receptor substrate-1 degradation is mediated by the proteasome degradation pathway. Diabetes **48:**1359-1364.
82. **Moncini S, Salvi A, Zuccotti P, Viero G, Quattrone A, Barlati S, de Petro G, Venturin M, Riva P.** 2011. The role of miR-103 and miR-107 in regulation of CDK5R1 expression and in cellular migration. PLoS ONE **6**.
83. **Moncini S, Bevilacqua A, Venturin M, Fallini C, Ratti A, Nicolin A, Riva P.** 2007. The 3′ untranslated region of human Cyclin-Dependent Kinase 5 Regulatory subunit 1 contains regulatory elements affecting transcript stability. BMC Molecular Biology **8**.
84. **Lee MS, Kwon YT, Li M, Peng J, Friedlander RM, Tsai LH.** 2000. Neurotoxicity induces cleavage of p35 to p25 by calpain. Nature **405:**360-364.
85. **Patrick GN, Zukerberg L, Nikolic M, De La Monte S, Dikkes P, Tsai LH.** 1999. Conversion of p35 to p25 deregulates Cdk5 activity and promotes neurodegeneration. Nature **402:**615-622.
86. **Asada A, Yamamoto N, Gohda M, Saito T, Hayashi N, Hisanaga SI.** 2008. Myristoylation of p39 and p35 is a determinant of cytoplasmic or nuclear localization of active cycline-dependent kinase 5 complexes. Journal of Neurochemistry **106:**1325-1336.
87. **Collombat P, Xu X, Heimberg H, Mansouri A.** 2010. Pancreatic beta-cells: From generation to regeneration. Seminars in Cell and Developmental Biology **21:**838-844.
88. **Lee KY, Helbing CC, Choi KS, Johnston RN, Wang JH.** 1997. Neuronal Cdc2-like kinase (Nclk) binds and phosphorylates the retinoblastoma protein. Journal of Biological Chemistry **272:**5622-5626.
89. **Hofmeister-Brix A, Lenzen S, Baltrusch S.** 2013. The ubiquitin-proteasome system regulates the stability and activity of the glucose sensor glucokinase in pancreatic β-cells. Biochemical Journal **456:**173-184.

90. **Schlesinger DH, Goldstein G.** 1975. Molecular conservation of 74 amino acid sequence of ubiquitin between cattle and man. Nature **255:**42304.
91. **Hershko A, Ciechanover A.** 1998. The ubiquitin system, p. 425-479, Annual Review of Biochemistry, vol. 67.
92. **Hershko A.** 2005. The ubiquitin system for protein degradation and some of its roles in the control of the cell division cycle. Cell Death and Differentiation **12:**1191-1197.
93. **Ciechanover A, Schwartz AL.** 2004. The ubiquitin system: Pathogenesis of human diseases and drug targeting. Biochimica et Biophysica Acta - Molecular Cell Research **1695:**3-17.
94. **Glickman MH, Ciechanover A.** 2002. The ubiquitin-proteasome proteolytic pathway: Destruction for the sake of construction. Physiological Reviews **82:**373-428.
95. **Ciechanover A, Orian A, Schwartz AL.** 2000. Ubiquitin-mediated proteolysis: Biological regulation via destruction. BioEssays **22:**442-451.
96. **Schwartz AL, Ciechanover A.** 1999. The ubiquitin-proteasome pathway and pathogenesis of human diseases, p. 57-74, Annual Review of Medicine, vol. 50.
97. **Lovering R, Hanson IM, Borden KLB, Martin S, O'Reilly NJ, Evan GI, Rahman D, Pappin DJC, Trowsdale J, Freemont PS.** 1993. Identification and preliminary characterization of a protein motif related to the zinc finger. Proceedings of the National Academy of Sciences of the United States of America **90:**2112-2116.
98. **Kawaguchi M, Minami K, Nagashima K, Seino S.** 2006. Essential role of ubiquitin-proteasome system in normal regulation of insulin secretion. Journal of Biological Chemistry **281:**13015-13020.
99. **Yan FF, Lin CW, Cartier EA, Shyng SL.** 2005. Role of ubiquitin-proteasome degradation pathway in biogenesis efficiency of β-cell ATP-sensitive potassium channels. American Journal of Physiology - Cell Physiology **289:**C1351-C1359.
100. **Hartley T, Brumell J, Volchuk A.** 2009. Emerging roles for the ubiquitin-proteasome system and autophagy in pancreatic β-cells. American Journal of Physiology - Endocrinology and Metabolism **296:**E1-E10.
101. **Bhatnagar S, Soni MS, Wrighton LS, Hebert AS, Zhou AS, Paul PK, Gregg T, Rabaglia ME, Keller MP, Coon JJ, Attie AD.** 2014. Phosphorylation and degradation of tomosyn-2 de-represses insulin secretion. Journal of Biological Chemistry **289:**25276-25286.
102. **Soleimanpour SA, Gupta A, Bakay M, Ferrari AM, Groff DN, Fadista J, Spruce LA, Kushner JA, Groop L, Seeholzer SH, Kaufman BA, Hakonarson H, Stoffers DA.** 2014. The diabetes susceptibility gene Clec16a regulates mitophagy. Cell **157:**1577-1590.
103. **Zhang W, Lilja L, Mandic SA, Gromada J, Smidt K, Janson J, Takai Y, Bark C, Berggren PO, Meister B.** 2006. Tomosyn is expressed in β-cells and negatively regulates insulin exocytosis. Diabetes **55:**574-581.
104. **Wang L, Luk CT, Schroer SA, Smith AM, Li X, Cai EP, Gaisano H, MacDonald PE, Hao Z, Mak TW, Woo M.** 2014. Dichotomous role of pancreatic HUWE1/MULE/ARF-BP1 in modulating beta cell apoptosis in mice under physiological and genotoxic conditions. Diabetologia **57:**1889-1898.

105. **Lemaire K, Moura RF, Granvik M, Igoillo-Esteve M, Hohmeier HE, Hendrickx N, Newgard CB, Waelkens E, Cnop M, Schuit F.** 2011. Ubiquitin fold modifier 1 (UFM1) and its target UFBP1 protect pancreatic beta cells from ER stress-induced apoptosis. PLoS ONE **6**.
106. **Yu P, Chen Y, Tagle DA, Cai T.** 2002. PJA1, encoding a RING-H2 finger ubiquitin ligase, is a novel human X chromosome gene abundantly expressed in brain. Genomics **79:**869-874.
107. **Lignitto L, Carlucci A, Sepe M, Stefan E, Cuomo O, Nistic√ ≥ R, Scorziello A, Savoia C, Garbi C, Annunziato L, Feliciello A.** 2011. Control of PKA stability and signalling by the RING ligase praja2. Nature Cell Biology **13:**412-424.
108. **Lignitto L, Arcella A, Sepe M, Rinaldi L, Delle Donne R, Gallo A, Stefan E, Bachmann VA, Oliva MA, Tiziana Storlazzi C, L'Abbate A, Brunetti A, Gargiulo S, Gramanzini M, Insabato L, Garbi C, Gottesman ME, Feliciello A.** 2013. Proteolysis of MOB1 by the ubiquitin ligase praja2 attenuates Hippo signalling and supports glioblastoma growth. Nature Communications **4**.
109. **Fredrickson EK, Candadai SVC, Tam CH, Gardner RG.** 2013. Means of self-preservation: How an intrinsically disordered ubiquitin-protein ligase averts self-destruction. Molecular Biology of the Cell **24:**1041-1052.
110. **Badciong JC, Haas AL.** 2002. MdmX is a RING finger ubiquitin ligase capable of synergistically enhancing Mdm2 ubiquitination. Journal of Biological Chemistry **277:**49668-49675.
111. **Ranaweera RS, Yang X.** 2013. Auto-ubiquitination of Mdm2 enhances its substrate ubiquitin ligase activity. Journal of Biological Chemistry **288:**18939-18946.
112. **Burns SM, Vetere A, Walpita D, Dančík V, Khodier C, Perez J, Clemons PA, Wagner BK, Altshuler D.** 2015. High-throughput luminescent reporter of insulin secretion for discovering regulators of pancreatic beta-cell function. Cell Metabolism **21:**126-137.
113. **Kawai H, Lopez-Pajares V, Kim MM, Wiederschain D, Yuan ZM.** 2007. RING domain-mediated interaction is a requirement for MDM2's E3 ligase activity. Cancer Research **67:**6026-6030.
114. **Hedrick ED, Agarwal E, Leiphrakpam PD, Haferbier KL, Brattain MG, Chowdhury S.** 2013. Differential PKA activation and AKAP association determines cell fate in cancer cells. Journal of Molecular Signaling**:**10.

Appendix

CDK5R1_S91A	CDK5R1_S91A_MG	CDK5R1	CDK5R1_MG	Gene Name
197	158	183	130	HECTD1 [BioGRID]
187	197	255	293	CDK5 [BioGRID]
168	140	209	210	CDK2 [BioGRID]
20		30	20	HUWE1 [BioGRID]
18		20		KPNA6 [BioGRID]
17		17	21	CDK1 [BioGRID]
13		43	23	VPRBP [BioGRID]
13	33	20	67	IPO4 [BioGRID]
12	25	27	30	CRCP [BioGRID]
7	12	25	13	SMYD2 [BioGRID]
7				MKLN1 [BioGRID]
7		8		CUL2 [BioGRID]
6				RBL2 [BioGRID]
	11	15	14	KPNA1 [BioGRID]
	8		9	DICER1 [BioGRID]
	5		6	PJA2 [BioGRID]
		33	35	USP7 [BioGRID]
		31	66	PRKAA1 [BioGRID]
		23	36	PRKAG1 [BioGRID]
		23		NAP1L4 [BioGRID]
		18		DCAF7 [BioGRID]
		18		PPM1G [BioGRID]
		16	13	SIRT1 [BioGRID]
		15		RPAP3 [BioGRID]
		15		KPNA3 [BioGRID]
		9	12	PRKAB1 [BioGRID]
		5		UBE2NL [BioGRID]
		5		E1A [BioGRID]
		4		STRN3 [BioGRID]
			34	ENO3 [BioGRID]
			27	HARS [BioGRID]
			17	POLR2E [BioGRID]
			9	PPP2R1B [BioGRID]
			7	PHKA2 [BioGRID]
			5	POLR3H [BioGRID]
			4	LONRF2 [BioGRID]

Appendix A. Candidate list of p35 (CDK5R1) interactor genes. Cells expressing FLAG-CDK5R1 (or mutant) were treated with MG132 or DMSO control followed by immunoprecipitation with anti-FLAG antibody and coupled with mass spectrometry to identify p35-interacting proteins. The list of interacting genes is presented on the right. The numbers indicate amount of peptides matches identified.

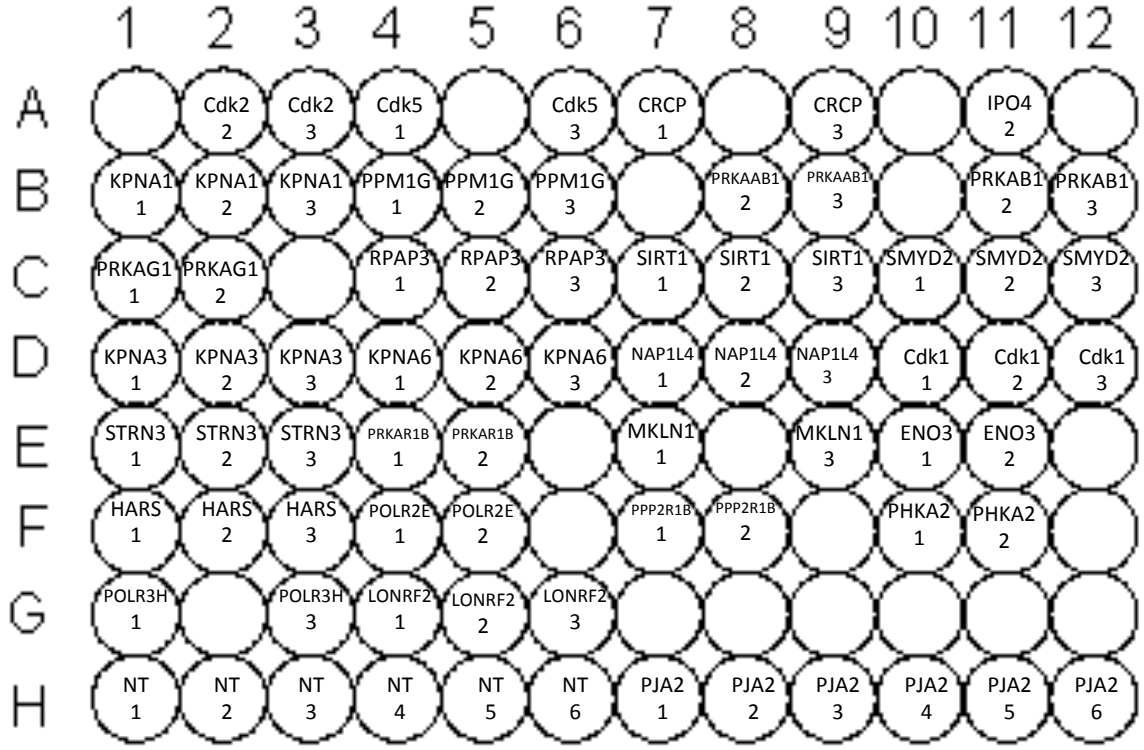

Appendix B. Outline of high-throughput RNAi screen 96-well plate format. Lentiviral encoding shRNA corresponding to candidate p35 interactor genes were arrayed in a 96-well tissue culture plates. Row H corresponds to non-targeting shRNA control and positive control shPJA2 which is known to elevate p35 levels. Empty spaces correspond to wells which do not have aliquoted virus.

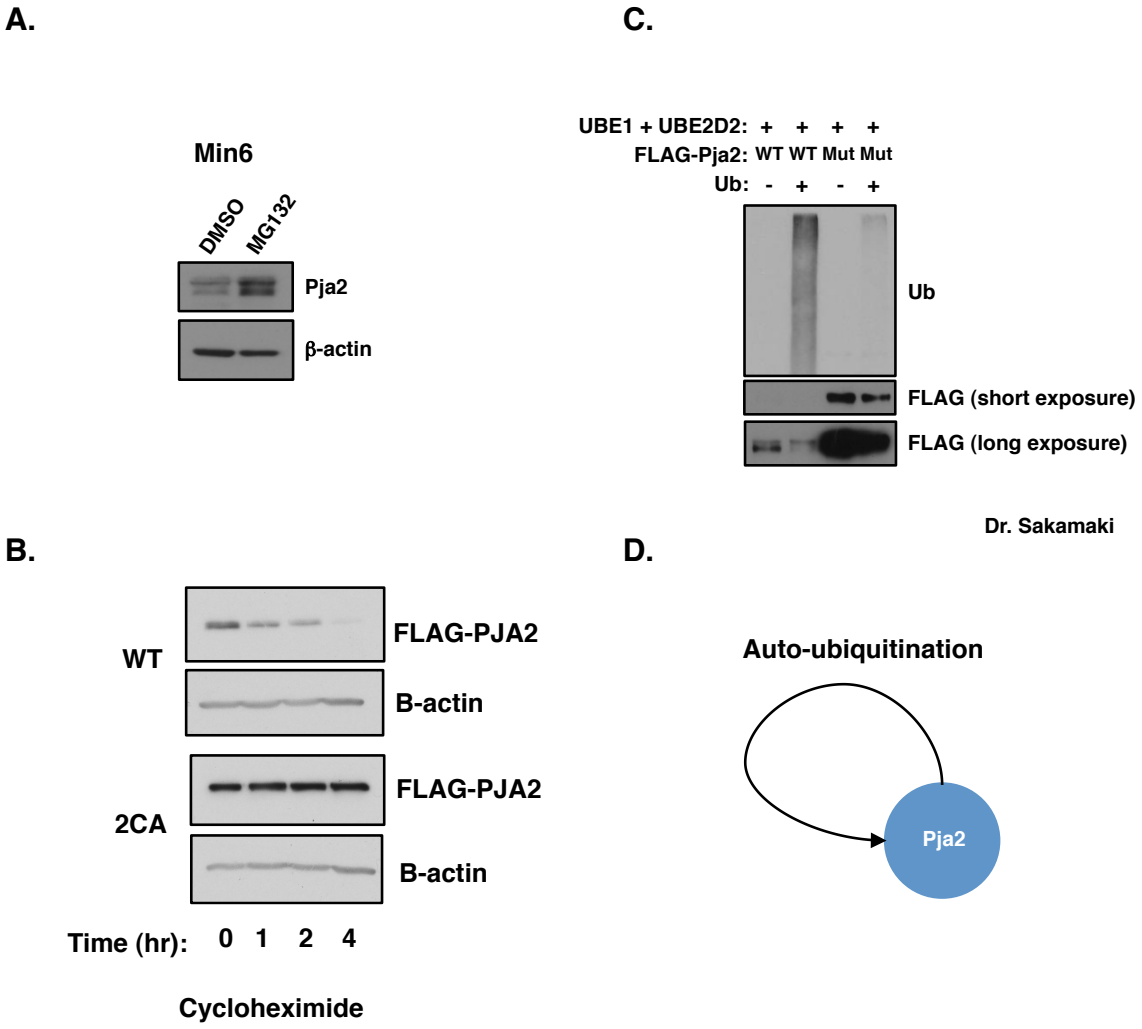

Appendix C. PJA2 undergoes auto-ubiquitination

(A) The effect of proteasomal inhibitor MG132 or DMSO control on MIN6 cells. **(B)** HEK 293T cells were transfected with wild-type PJA2 or 2CA mutant for 48 hr prior to treatment with cycloheximide. Cells were harvested at the indicated time-points to monitor FLAG-PJA2 levels. **(C)** In vitro auto-ubiquitination assay of wild-type or 2CA (Mut) PJA2. **(D)** Schematic depicting PJA2 undergoing auto-ubiquitination.

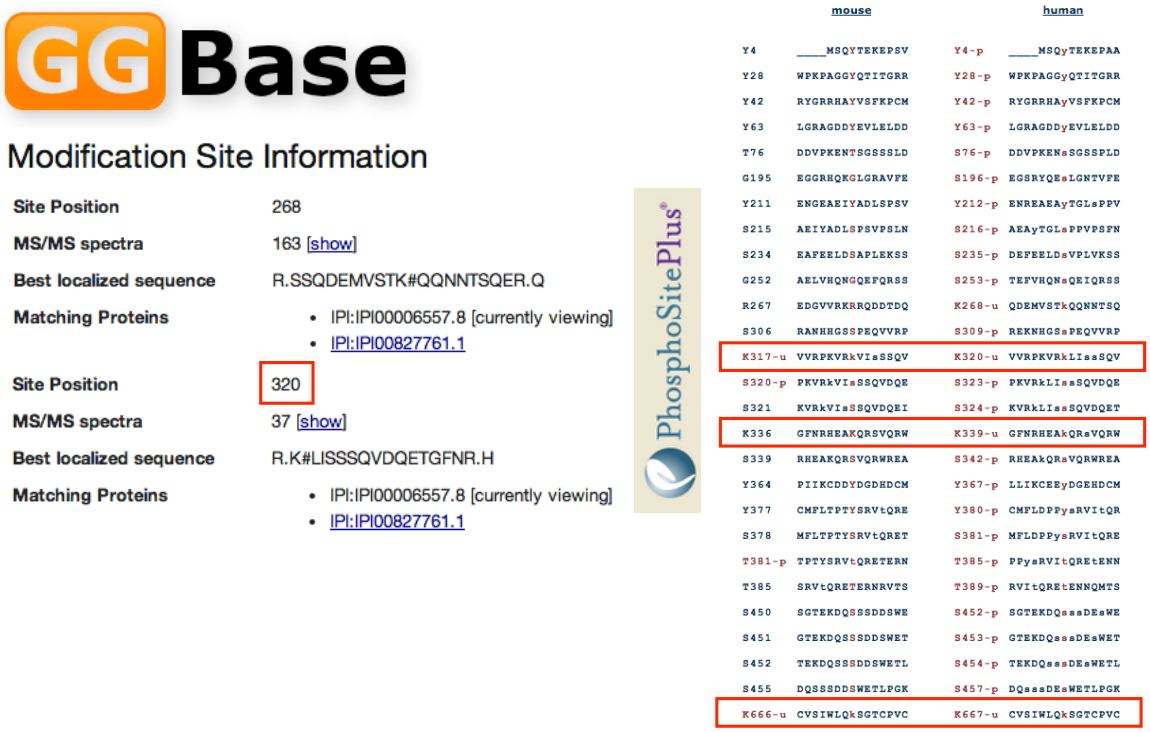

Appendix D. Post-translational modification databases GGBase and Phosphosite report on PJA2 ubiquitination sites K317, K336, and K666. GGbase reports on two ubiquitination sites of PJA2 of which only Lys 320 (left) is conserved between humans and mice. Phosphosite also reports on 3 lysine residues reported to undergo ubiquitination (right) which are conserved in both humans and mice.

Conserved Lysine Residues in PJA2

Appendix E. RING Domain of PJA2 is highly conserved between the above-specified species. PJA2 amino acid sequences were obtained from Uniprot before alignment with the tool ClustalW2. The conserved lysine residues are highlighted in yellow.

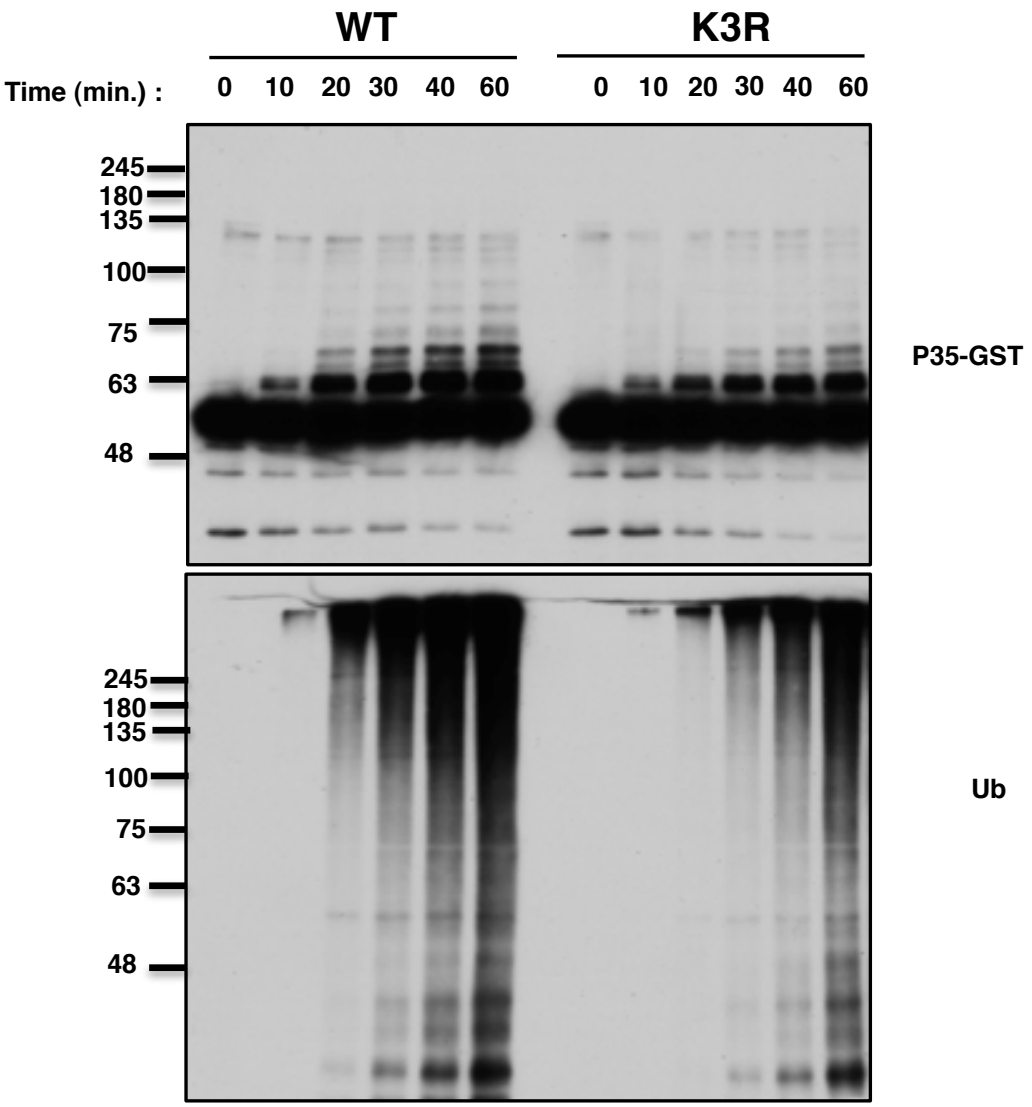

Appendix F. PJA2 K3R mutant is functional and demonstrates similar enzymatic kinetics as wild-type PJA2. In vitro ubiquitination time-course assay testing wild-type PJA2, 2CA and K3R mutant ability to ubiquitinate GST-p35 substrate. Samples were incubated at 37°C and aliquots were removed after each time point and mixed with equal volume of 2X SDS before separation by SDS-PAGE and subsequent blotting for p35 and ubiquitin.

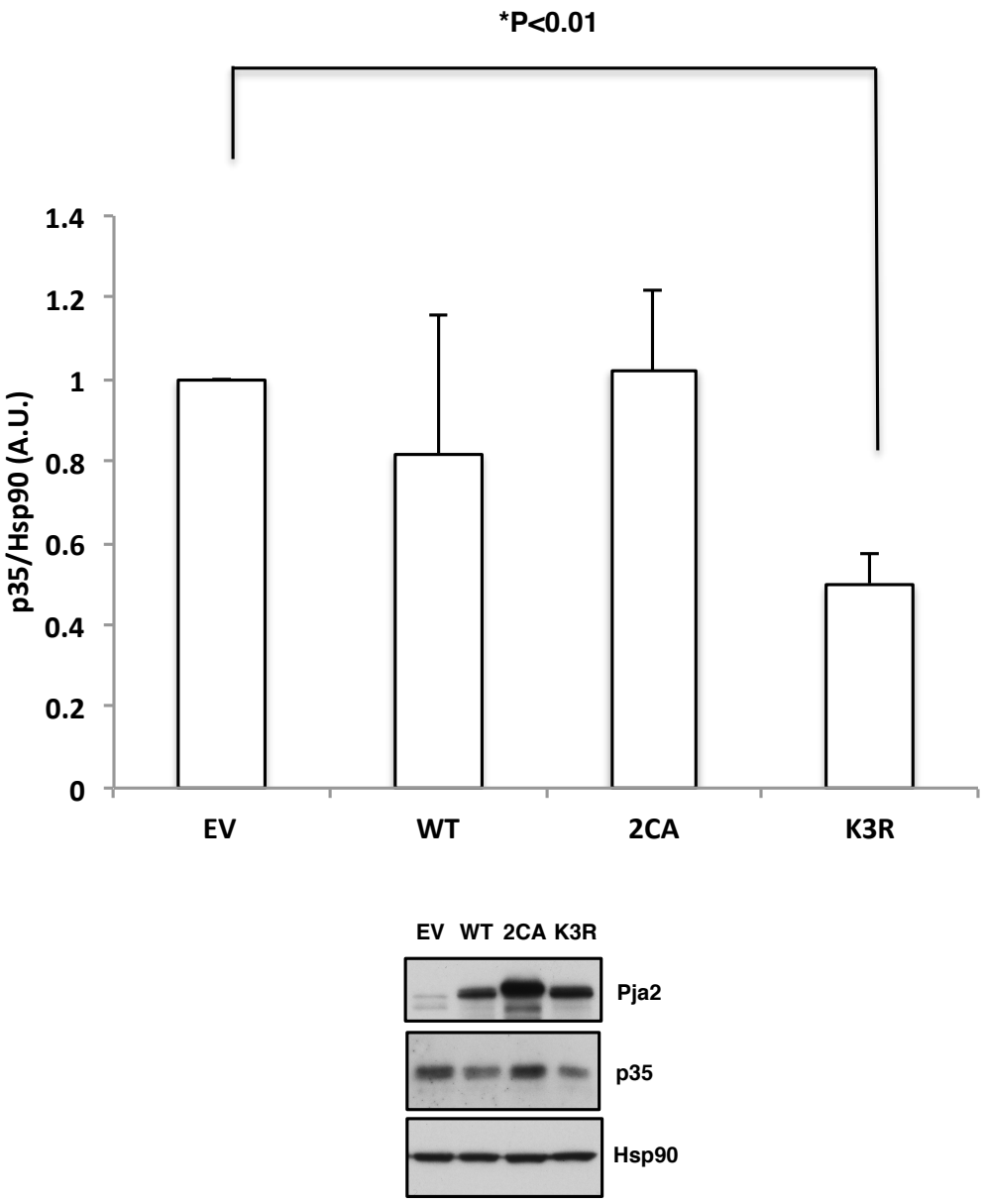

Appendix G. Overexpression of PJA2 K3R mutant significantly reduces endogenous p35 levels in MIN6 cells. Min6 cells were infected for 72 hr with lentivirus overexpressing either empty vector control (EV) or PJA2 constructs (wild-type, 2CA, or K3R). Cells were harvested and lysed before separating by SDS-PAGE. Densitometry of p35 levels was assessed after normalizing to the internal control of HSP90. Statistics are representative of 3 independent experiments.

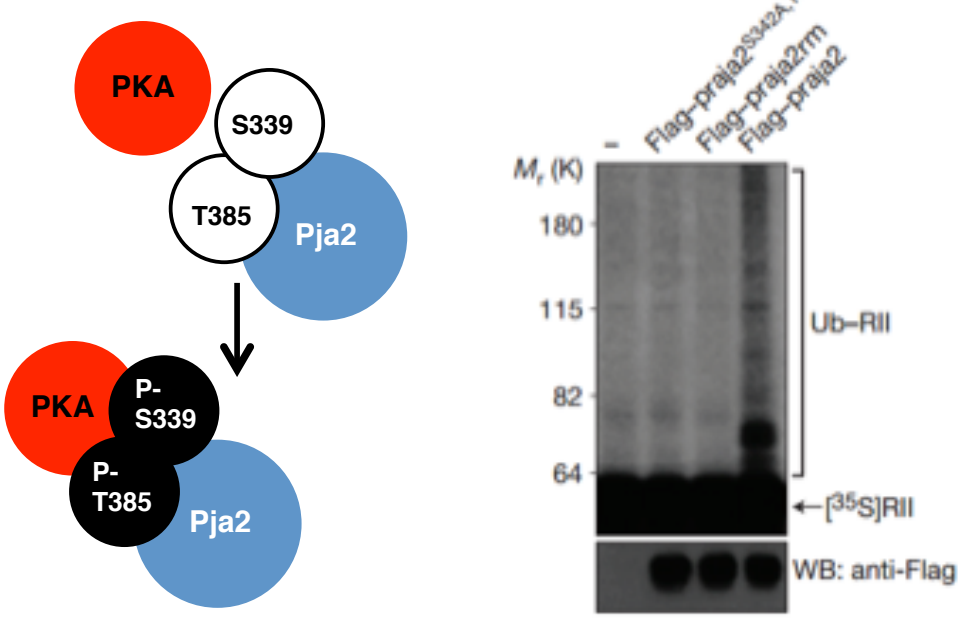

Lignitto et al. 2011

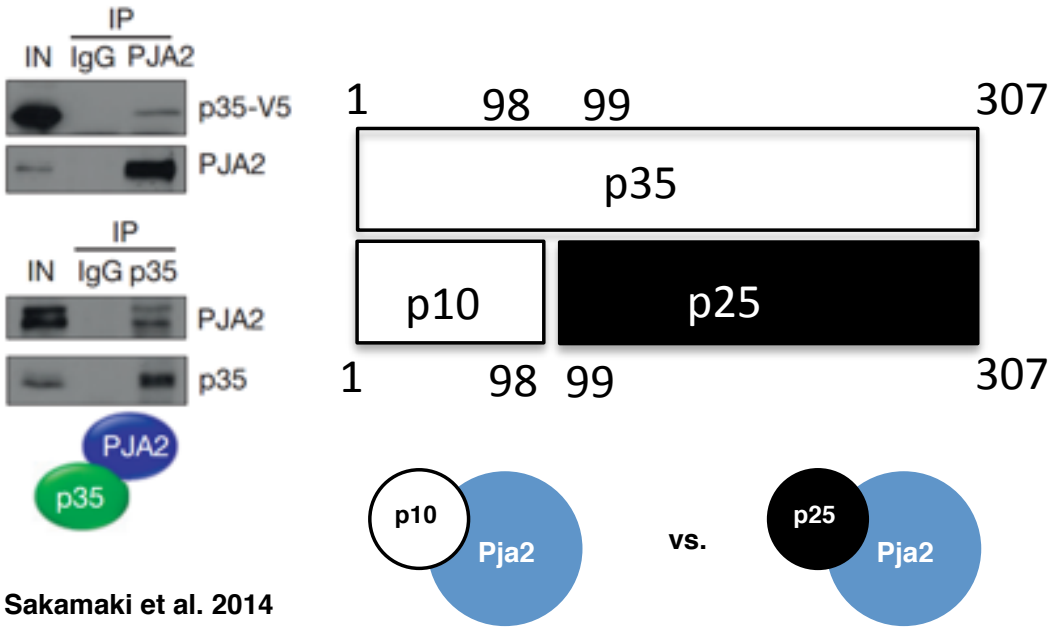

Sakamaki et al. 2014

Appendix H: The E3 ligase PJA2 interacts with p35
Co-immunoprecipitation experiments demonstrate that endogenous PJA2 can CO-IP with overexpressed p35-V5 (above) and that endogenous p35 is able to immunoprecipitate endogenous PJA2 (below). Schematic representation of p35 protein as well as p10 and p25 fragments.

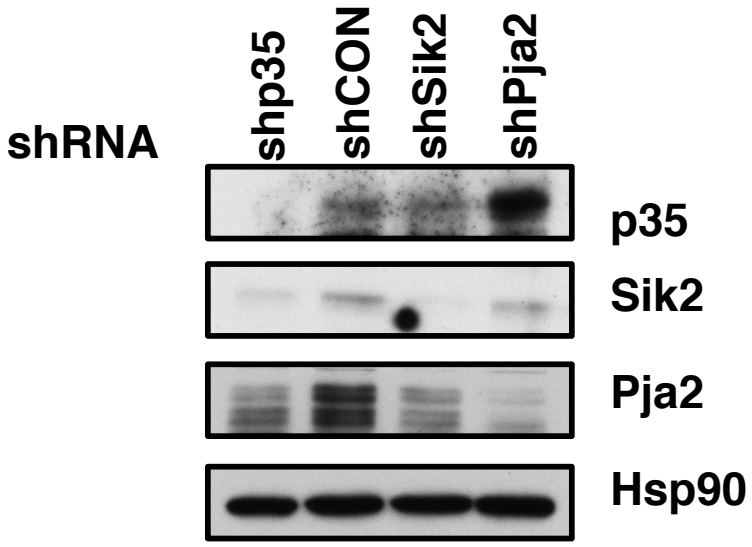

Appendix I. Characterizing PJA2 protein levels after knockdown of shp35, shCON, shSIK2, and shPJA2 control. Min6 cells were infected for 72 hr with lentivirus expressing shp35, shCON, shSIK2, and shPJA2 prior to harvesting for western analysis.

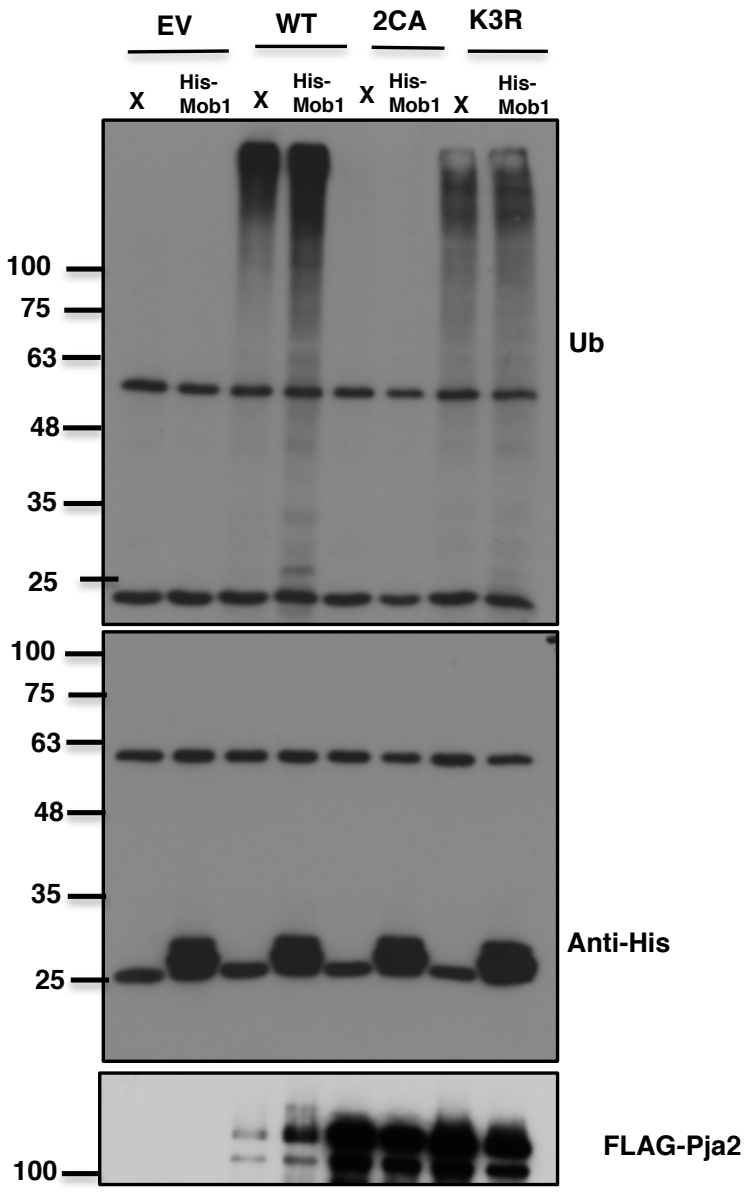

Appendix J. In vitro ubiquitination assay with PJA2 constructs and MOB1 substrate. In vitro ubiquitination assay testing wild-type PJA2, 2CA and K3R mutant ability to ubiquitinate His-MOB1 substrate. Samples were incubated at 37°C for 1 hr prior to addition of equal volume 2X SDS before separation by SDS-PAGE and subsequent blotting for His-MOB1, ubiquitin, and FLAG-PJA2.